



universität
wien

DIPLOMARBEIT

Titel der Diplomarbeit

Over-expression of Fibroblast Growth Factor 5 (FGF5)
in Melanoma:

Evaluation of its Role in Tumor Progression and
Potential Therapeutic Implications

Verfasserin

Mag. Sara Ghassemi

angestrebter akademischer Grad

Magistra der Naturwissenschaften (Mag.rer.nat.)

Wien, 2011

Studienkennzahl lt. Studienblatt:

A 441

Studienrichtung lt. Studienblatt:

Diplomstudium Genetik – Mikrobiologie

Betreuerin / Betreuer:

Ao. Univ. Prof. Dr. Christian Seiser

**This diploma thesis was conducted at the
Medical University of Vienna, Department of
Medicine I, Institute of Cancer Research**

Supervisor:

Priv. Doz. Dr. Michael Grusch

***This thesis is dedicated to my wonderful parents for their endless love and
for supporting me in all ways Imaginable.***

Acknowledgements

I would like to acknowledge several people for the completion of this thesis. I did not achieve this level of success alone. My special thanks go to Dr. Grusch for enabling me to perform this thesis at his laboratory and his ongoing support and guidance.

I would like to acknowledge Prof. Dr. Seiser for mentoring my thesis. I thank my lab mates, Emine and Julia for creating a friendly working atmosphere and their encouragement.

I express my sincere thanks to the FGF group members Prof. Dr. Walter Berger, Prof. Dr. Brigitte Marian, Prof. Dr. Bettina Grasl-Kraupp, Prof. Dr. Klaus Holzmann, and Mag. Christine Heinzle for all their support.

I would like to thank Mag. Markus Mandl from the group of Prof. Dr. Karin Macfelda Dept. of Biomedical Research, Medical University of Vienna for his cooperation.

Zusammenfassung

Das kutane maligne Melanom ist ein Tumor mit steigender Inzidenz, der aus pigmentproduzierenden Melanozyten entsteht. Im Frühstadium der Erkrankung ist durch eine Operation eine vollständige Heilung möglich. Haben sich jedoch bereits Metastasen in anderen Organen gebildet, steht bisher keine kurative Therapie zur Verfügung.

FGF/FGFR Signalsysteme spielen bei zahlreichen Tumorarten eine entscheidende Rolle im Zellwachstum und -überleben und in der Angiogenese. Die Überexpression von Fibroblasten-Wachstumsfaktor 2 (FGF2) und Mutationen in Signaltransduktionswegen wie BRAF sind die charakteristischen Merkmale von Melanomzellen. Expressionsanalysen zeigten Überexpression von FGF5 in 90% der untersuchten Melanomzelllinien, während FGF5 von gesunden Melanozyten praktisch nicht gebildet wird.

Ziele: Die Ziele der Arbeit waren: A) Untersuchung der Auswirkungen von FGF5 Überexpression und Inhibierung auf den malignen Phänotyp von Melanomzellen *in vitro*. B) Analyse der Wirkung von FGF5 Überexpression auf das Tumorstadium *in vivo* durch Xenotransplantationsexperimente in SCID-Mäusen.

Methoden: Die Experimente umfassten: (I) Generation von isogenen Zellmodellen mit Überexpression von FGF5, (II) Analyse der Auswirkungen der FGF5 Überexpression auf den malignen Phänotyp *in vitro*, (III) Analyse des Effekts der FGF5 Überexpression auf das Tumorstadium *in vivo*, (IV) Etablierung von shRNA-induziertem Knockdown des endogenen FGF5 mittels Lentiviren und Untersuchung der Auswirkungen des Knockdowns *in vitro*, (V) Analyse der Wirkung eines Extrakts der Heilpflanze *Neurolena lobata* auf Melanomzellwachstum und FGF/FGFR-Expression.

Resultate: Ergebnisse des Scratch Assay sowie des Invasion Assay zeigten deutlich den Einfluss der FGF5 Überexpression auf eine gesteigerte Migrationsfähigkeit der VM1 Zelllinie. Eine erhöhte Klonogenität wurde in VM1 Zellen mit FGF5 Überexpression im Vergleich zu GFP Kontrolle ebenfalls beobachtet. Keine signifikante Wirkung von FGF5 Überexpression wurde im Soft Agar Assay

beobachtet. Weiters wurde gezeigt, dass Überexpression von FGF5 keine Auswirkung auf die Proliferation von VM1 und VM21 Zellen *in vitro* hat.

Ergebnisse der Xenotransplantations Experimente in SCID-Mäusen haben gezeigt, dass Zellen mit FGF5 Überexpression früher Tumore bilden und eine Erhöhung der Tumorgroße im Vergleich zu Kontrollen aufweisen. Eine hohe Rate der Zellproliferation vor allem an den Tumorrändern wurde durch Ki-67 Färbungen nachgewiesen. Endothelzellen wurden durch Färbung mit vonWillebrand-Faktor identifiziert. In HE und Ki-67 Färbungen der Lunge und Leber von Mäusen wurden jedoch weder in der FGF5 überexprimierenden Gruppe noch in der Kontrollgruppe Metastasen aus den xenotransplantierten Tumoren beobachtet.

Ein shRNA-vermittelten Knockdown des endogenen FGF5 zeigte eine hemmende Wirkung auf die Koloniebildung *in vitro*, hatte aber keine Auswirkung auf die Migrationsfähigkeit der Zellen.

Ergebnisse der Behandlung von Melanomzellen mit *N. lobata* Extrakt zeigten eine konzentrationsabhängige zytotoxische Wirkung in allen getesteten Melanomzelllinien. Eine Reduktion der Expression von FGF2 nicht jedoch von FGFR1 oder 4 wurde in den mit *N. lobata* Extrakt behandelten Zellen beobachtet.

Schlussfolgerungen: Eine stimulierende Wirkung von FGF5 auf maligne Eigenschaften von Melanomzellen konnte sowohl *in vitro* als auch *in vivo* gezeigt werden.

Abstract

Cutaneous malignant melanoma is a tumor derived from pigment producing melanocytes with rising incidence. Curative treatment of melanoma is possible only at an early stage, when complete surgical removal of the tumor is possible and once metastasis has occurred, no curative therapy exists.

FGF/FGFR signaling systems play a critical role in tumor cell growth, survival and angiogenesis of several tumor types. Over-expression of fibroblast growth factor 2 (FGF2) and mutations in signal transduction pathway molecules like BRAF are characteristic features of melanoma cells.

Objectives: The purpose of the study was: A) Investigating the effects of FGF5 over-expression and knock down on the malignant phenotype of melanoma cells *in vitro*. B) Analyzing the effect of FGF5 over-expression on tumor growth *in vivo* by xenotransplantation experiments in SCID mice.

Methods: The thesis included (I) Generation of isogenic cell models over-expressing FGF5, (II) Analysis of the Impact of FGF5 over-expression on the malignant phenotype of melanoma cells *in vitro*, (III) Analysis of FGF5 over-expression on tumor growth *in vivo*, (IV) Generation of lentiviral shRNA-mediated knock down of endogenous FGF5 and investigating the impact of down modulation of endogenous FGF5 *in vitro*, (V) Analysis of the effect of an extract from the medicinal plant *Neurolena lobata* on melanoma cell growth and FGF/FGFR expression.

Results: Results of the scratch assay as well as the invasion assay showed clearly the influence of FGF5 over-expression to result in a more migratory phenotype in the VM1 cell line. An increased clonogenicity was also observed in VM1 cells with FGF5 over-expression compared to GFP controls. No significant impact on the ability of cells expressing FGF5 to form clones in soft agar was observed in contrast to cells with the GFP construct. Relating to effects of FGF5 over-expression on proliferation of VM1 and VM21 cells *in vitro*, no difference was observed compared to GFP over-expressing cells.

Results of xenotransplantation experiments in SCID mice showed that cells with FGF5 formed palpable tumors earlier and tumor volume was increased in contrast to mock transfected controls. A high rate of cell proliferation especially at the tumor

margins was demonstrated by Ki-67 staining. Endothelial cells were identified by staining for vonWillebrand factor. The occurrence of metastasis was observed neither in the FGF5 over-expressing nor in the control group when analyzed by HE and Ki-67 staining of lungs and livers of the mice.

ShRNA-mediated knock down of endogenous FGF5 showed an inhibitory effect on colony formation *in vitro*, but had no effect on the migration ability of the cells.

Treatment of melanoma cells with *N. lobata* extract led to dose-dependent cytotoxicity. A reduction in FGF2 expression was detected after treatment with *N. lobata* extract, while no difference in expression of FGFR1 and FGFR4 was observed.

Conclusion: A stimulating effect of FGF5 on the malignant phenotype of melanoma cells could be demonstrated *in vitro* and *in vivo*.

Table of Contents

1	<i>Aim of the Study</i>	11
2	<i>Introduction</i>	12
2.1	Cellular and molecular biology of melanoma	12
2.2	Homeostatic imbalance and dysplastic nevi	13
2.3	Genetic aberrations and melanoma progression	14
2.4	Fibroblast growth factors (FGF) and FGF-receptors	17
2.4.1	Evolution of the FGF and FGFR gene family	17
2.4.2	Structural and functional properties of FGFs and FGF-receptors	18
2.4.3	FGF-receptors (FGFRs)	20
2.4.4	Dysregulation of FGF signaling in cancer	22
3	<i>Materials and Methods</i>	26
3.1	Cell lines and media	26
3.2	Standard growth conditions	26
3.3	Splitting	26
3.4	Cell counting	27
3.5	Freezing	27
3.6	Isolation of RNA	27
3.7	Determination of RNA concentration	27
3.8	Synthesis of cDNA	28
3.9	TaqMan - “Real Time” quantitative RT-PCR (qRT-PCR)	28
3.10	Gel electrophoresis (Nucleic acids)	29
3.11	Isolation of proteins	29
3.12	Determination of protein concentration	29
3.13	SDS-polyacrylamid gel electrophoresis	30
3.14	Western blot	31
3.15	Lipofection	32
3.16	Selection of stable transfectants	32
3.17	FACS sorting of GFP-positive stable clones	33
3.18	Lentiviral transduction	34
3.19	Cell viability assay (MTT assay)	34
3.20	Clonogenic assay	35
3.21	Crystal violet staining	35
3.22	Growth curve	35
3.23	Invasion assay	35
3.24	Soft agar assay	35
3.25	Hen’s egg test – chorionallantoic membrane (HET-CAM) assay	36

3.26	Tumor growth in SCID mice.....	37
3.27	Hematoxylin and eosin staining	37
3.28	Ki-67 immunohistochemistry	37
3.29	Von Willebrand Factor (vWF) antibody staining	38
3.30	Statistical analysis	38
4	Results	39
4.1	Expression analysis of fibroblast growth factor 5	39
4.2	Generation of isogenic cell models	39
4.3	Impact of FGF5 on the malignant phenotype of VM1 and VM21 <i>in vitro</i>	40
4.3.1	MTT assay.....	40
4.3.2	Growth curves.....	41
4.3.3	Clonogenic assay	42
4.3.4	Soft agar assay	43
4.3.5	Scratch assay.....	44
4.3.6	Invasion assay	46
4.4	HET-CAM assay (<i>ex vivo</i>).....	47
4.4.1	Immunohistochemical staining of hen's egg CAM.....	48
4.5	<i>In vivo</i> tumor growth	49
4.5.1	Immunohistochemical staining of VM21 xenograft tumors	50
4.6	HE staining of organs from mice engrafted with VM21-FGF5 or VM21-GFP	51
4.7	Lentiviral shRNA-mediated knockdown of endogenous FGF5	52
4.8	Impact of down-modulation of endogenous FGF5 <i>in vitro</i>	54
4.8.1	Effect of shRNA-mediated FGF5 down modulation on proliferation and viability of cells.	54
4.8.2	Effect of siRNA-mediated FGF5 down-modulation on clonogenicity.....	55
4.8.3	Effect of shRNA-mediated FGF5 down-modulation on invasion of cells	56
4.9	Treatment of melanoma cells with <i>Neurolena lobata</i> extract.....	58
4.9.1	Effect of <i>N. lobata</i> on FGF/FGFR expression	59
5	Discussion	61
5.1	Impact of FGF5 on the malignant phenotype <i>in vitro</i>	62
5.2	Hen's egg chorioallantoic membrane (HET-CAM)	62
5.3	Lentiviral shRNA-mediated knockdown of endogenous FGF5.....	63
5.4	<i>In vivo</i> tumor growth	63
5.5	Treatment of melanoma cells with <i>Neurolena lobata</i> extract.....	64
6	Appendix.....	65
6.1	List of Figures	65
6.2	List of Tables.....	67
6.3	Abbreviations	68
6.4	References.....	69
6.5	Curriculum Vitae.....	74

1 Aim of the Study

From previous data on FGF5 expression in melanoma and its role in astrocytic brain tumors it is hypothesized that over-expression of FGF5 contributes to melanoma growth and spreading by autocrine and paracrine activities facilitating angiogenesis and metastasis. Targeting FGF5-dependent signals may consequently offer novel therapeutic alternatives for combating melanoma.

The aim of this thesis was therefore to investigate the impact of FGF5 on tumor progression of melanoma and evaluate its potential implications for prognosis and therapy. For that purpose I analyzed:

- The effects of FGF5 over-expression and knock down on the malignant phenotype of melanoma cells *in vitro* with regard to proliferation, inhibition of cell death, migration, invasion and induction of angiogenesis.
- The effect of FGF5 expression on tumor growth *in vivo* by a xenotransplantation experiment in SCID mice.
- The impact of *Neurolena lobata* extract on FGF/FGFR expression in melanoma cells.

2 Introduction

2.1 Cellular and molecular biology of melanoma

Melanocytes are found in a wide variety of human tissues. They appear in the skin, but also in the eye, the meninges of the brain, in the heart and in bone. The color of the eyes depends on the quantity, quality, and distribution of the pigment melanin, which occurs in two types: black to brown eumelanin and yellow to reddish pheomelanin [1]. In the skin melanocytes are located in the germinal layer of the epidermis and determine skin color (Figure1) [2, 3].

Within the epidermis, melanocytes reside in the basal layer in a ratio of about 10 keratinocytes to 1 melanocyte [4]. It has been estimated that each melanocyte is in contact with 40 nearby keratinocytes. Through a process called melanogenesis, melanocytes produce melanin and supply it via dendrites to surrounding keratinocytes.

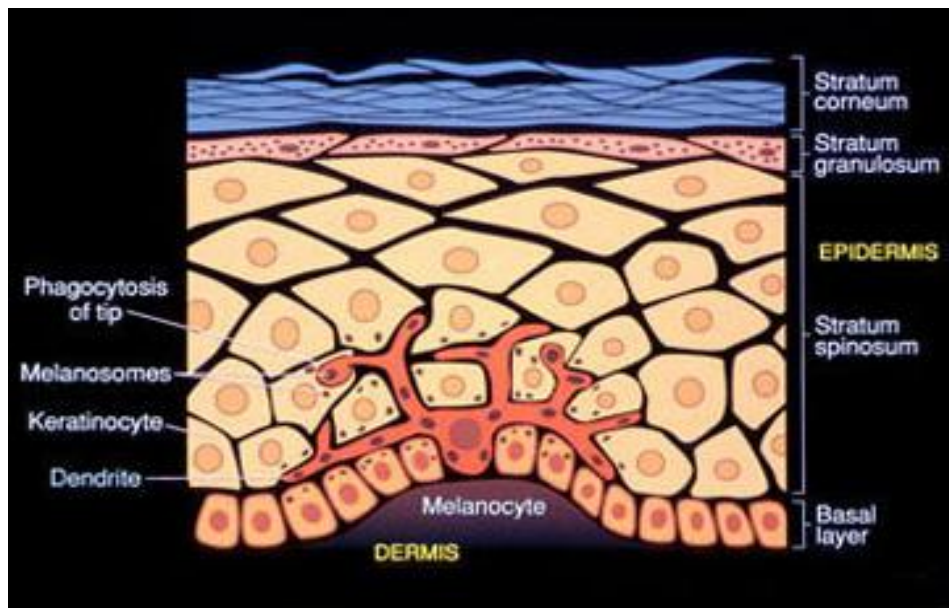


Figure 1: Location of melanocytes and keratinocytes in human skin [4].

UV is one of the major environmental factors, which causes an increase in melanin production. Melanin has a function as potent free radical scavenger in humans, protecting the DNA of skin cells from reactive oxygen species (ROS) that can be formed as a first consequence of UV exposure in high concentrations [5, 6].

Under normal condition in the skin, there is a homeostatic balance between melanocytes and surrounding cells. Keratinocytes control melanocyte growth and

behaviour through a complex system of paracrine growth factors and cell–cell adhesion molecules.

A change of epistasis is thought to be the entry point of melanoma development and is achieved by environmental, genetic as well as by epigenetic alterations in the skin tissue (Figure 2) [7].

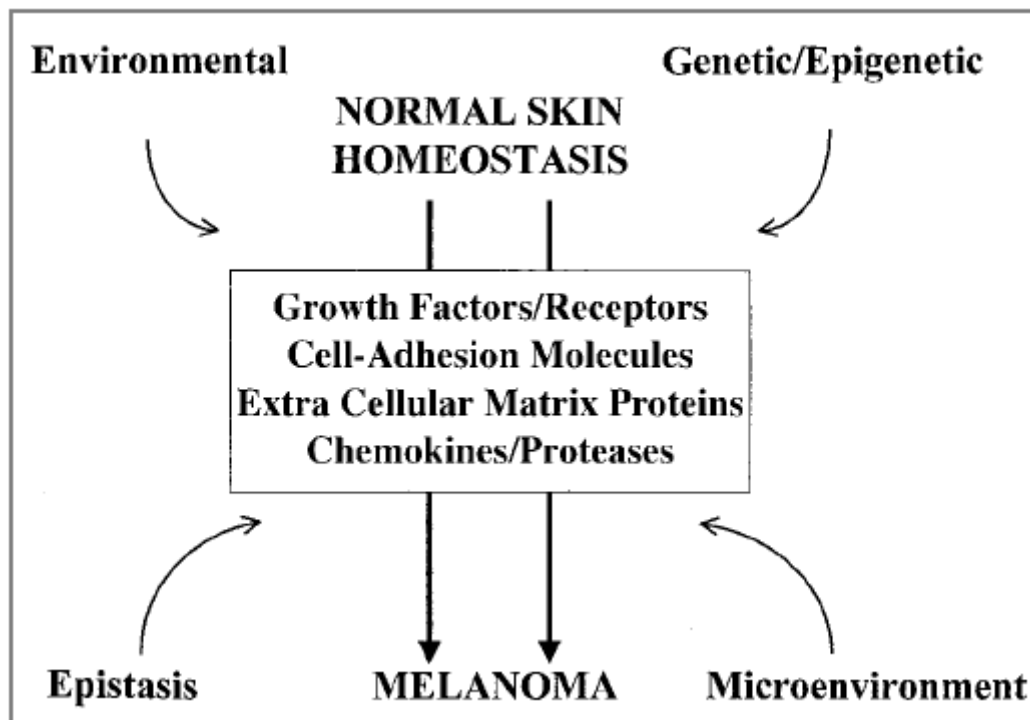


Figure 2: Factors suggested to influence melanoma development [8].

2.2 Homeostatic imbalance and dysplastic nevi

Alteration of homeostatic balance can lead to altered expression of cell–cell communication molecules and to development of melanoma. Melanocytes acquire the ability to express specific cell surface molecules allowing them to adhere to each other, survive, grow and migrate [2].

In the normal skin condition melanocytes and keratinocytes express E-cadherin, which mediates the communication and adhesion between melanocytes and keratinocytes [8, 9]. Disruption in E-cadherin and separation of melanocytes and keratinocytes appears to be one of the earliest steps in melanoma progression [10, 7]. On the other hand it is suggested that N-cadherin on melanoma cells is a major inductor for the formation of a dysplastic nevus and facilitates interaction with endothelial cells as well as fibroblasts. Beside N-cadherin, up-regulation of Mel-CAM receptor and zonula occludens protein-1 (ZO-1) are involved in melanoma-

melanoma interactions and melanoma progression (Figure 3) [2]. During melanoma progression there is a cadherin subtype switch from E- to N-cadherine which creates a milieu favoring tumor formation and invasion.

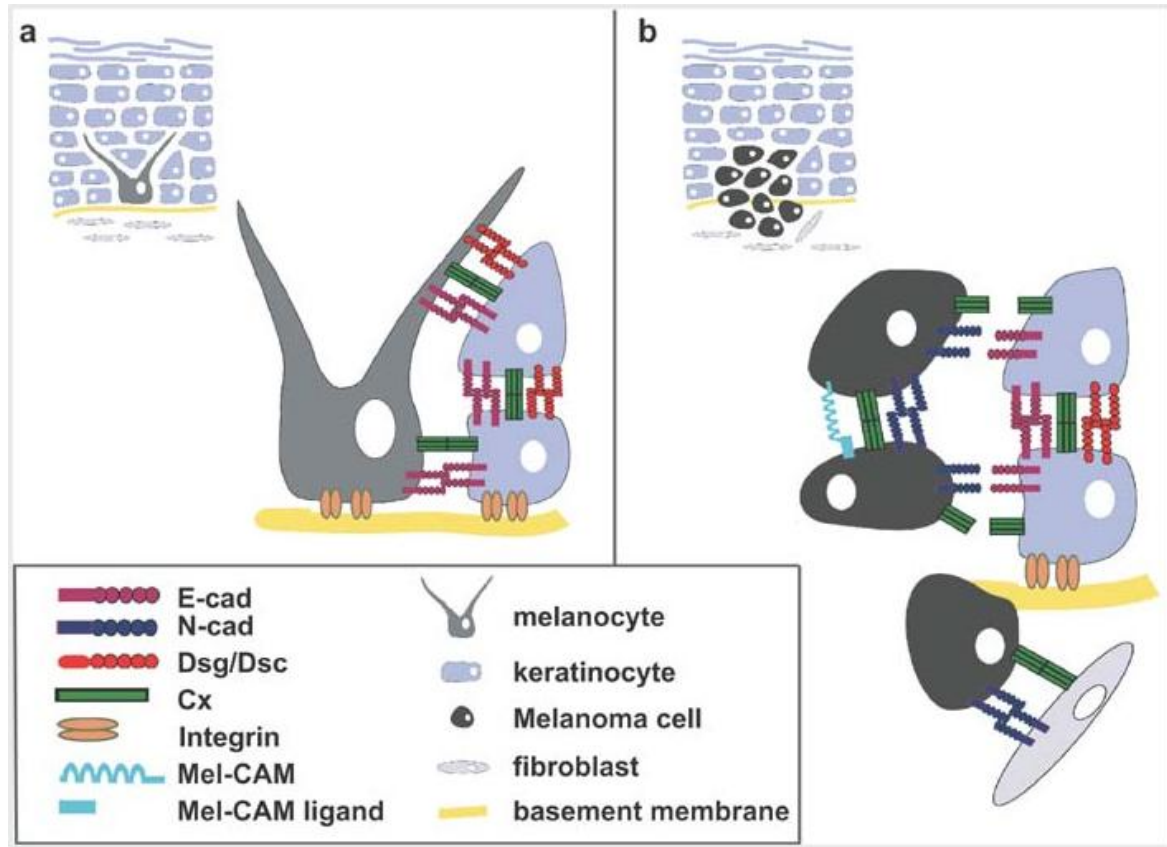


Figure 3: Dynamics of intercellular interactions under normal and pathological situations during melanoma development. (a) Normal melanocytes reside close to the basement membrane and form an 'epidermal melanin unit' that contains one melanocyte and five to eight keratinocytes. Melanocytes interact with adjacent keratinocytes through E-cadherin, desmoglein 1, and connexins. This contact-dependent interaction is required for the growth and phenotypic control of melanocytes by keratinocytes. (b) Malignant melanoma cells proliferate, penetrate basement membrane, and invade into dermis. A shift of cadherin profile from E to N during melanoma development not only frees the cells from epidermal keratinocytes, but also confers new adhesive properties. Melanoma cells form N-cadherin-mediated adhesion and connexin-mediated gap junctions with N-cadherin-expressing fibroblasts, endothelial cells, and adjacent melanoma cells. Mel-CAM and its unknown ligand are also involved in melanoma-melanoma cell interaction, which is implicated to play a role in the progression of melanoma [11].

2.3 Genetic aberrations and melanoma progression

Senescence is the loss of the ability to proliferate after a finite number of divisions. Once the cells overcome this barrier of cell senescence, they become neoplastic, immortal and aggressive [12]. Concerning melanoma it is known that INK4A, CDK4 and ARF are three melanoma susceptibility genes which are involved in the process of cellular senescence. The INK4a/ARF/INK4b locus (known as CDKN2a and CDKN2b) on chromosome 9p21 is deleted in many cancers including melanoma. This locus encodes three genes ARF (also known as p19ARF and p14ARF),

p15^{INK4b} and p16^{INK4a}. p15^{INK4b} and p16^{INK4a} have a function as inhibitors of the cyclin-dependent kinases, CDK4 and CDK6, which promote proliferation. Mutations in p16^{INK4a} gene were found in less than 25% of melanomas [13]. ARF as a tumor suppressor has the ability to bind and inactivate the MDM2 protein resulting in p53 stabilization [14]. Mutations in the tumor suppressor gene p53 are very rare in melanoma, less than 5% despite extreme chemoresistance of melanoma. One explanation for this paradox is that p53 function could be disabled by lesions that disrupt other components of the pathway that may also contribute to compromise the apoptotic process [15]. Up-regulation of anti-apoptotic factors (members of the Bcl-2 family) and down-modulation of pro-apoptotic genes (Apaf-1) are frequent in human melanoma [16]. For example, Apaf-1 (apoptotic protease activating factor-1) is a downstream effector of p53 which induces apoptosis in the presence of DNA damage. Down-regulation of this protein in cells reduced p53-dependent apoptosis and mediated oncogenic transformation. Decreased expression of Apaf-1 seen in correlation with melanoma progression could be interpreted as an event contributing to melanoma chemoresistance [15].

Activating mutations in the oncogene B-RAF are found in up to 80% in benign naevi and almost 70% of melanomas [17]. Mutations in B-Raf lead to downstream activation of the Mitogen Activated Protein Kinase/Extracellular Regulated Kinase (MAPK/ERK) pathway, which in turn down-regulates the proapoptotic proteins BIM and BAD leading to increased resistance to apoptosis.

The presence of a c-kit-activating mutation in metastatic malignant melanoma suggests that a small number of melanomas may progress by a somatic mutation of the c-kit gene [18]. Somatic mutations in NRAS have been found in ~ 13-25% of all malignant melanomas [19, 20, 21].

Result of these mutations is constitutive activation of NRAS signaling pathways. NRAS mutations are found in all melanoma subtypes, but may be slightly more common in melanomas derived from chronic sun-damaged (CSD) skin [19, 21]. In the vast majority of cases, NRAS mutations are non-overlapping with other oncogenic mutations found in melanoma (i.e. B-RAF mutations, c-kit mutations, etc.). Akt/PKB is a core component of the PI3K signaling pathway. Several studies have shown that activation of the Akt/PKB pathway induced the transcription of a wide range of genes, especially those involved in cell proliferation, apoptosis and cell survival [22]. HGF/SF and IGF-I are two growth factors which are secreted by

melanoma cells and surrounding stroma contributing to activate Akt/PKB signaling in an autocrine and paracrine manner [23, 24] and leading to increased proliferation (Figure4).

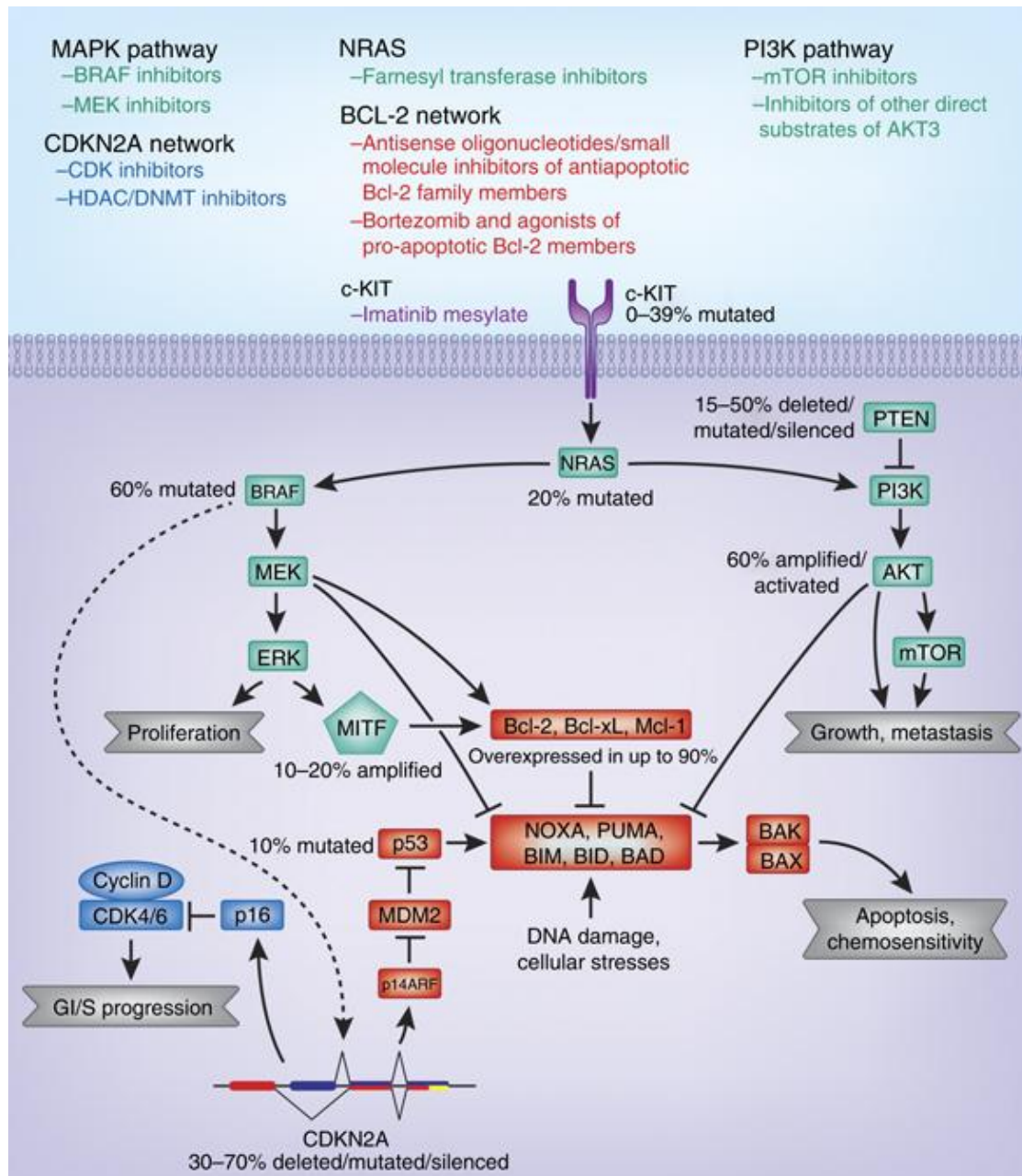


Figure 4: Melanoma signaling networks. Shown is a simplified diagram of three of the major genetic networks involved in melanoma tumorigenesis, survival, and senescence. Included in the NRAS signaling network (green) are the MAPK and the PI3 Kinase/AKT pathways, which have been implicated in melanoma proliferation, survival, and progression. The CDKN2A locus encodes two separate tumor suppressors, p16 and p14ARF, both of which are thought to contribute to senescence and tumor growth restriction. The p53/Bcl-2 signaling network (red) is a major contributor to melanoma apoptosis and chemosensitivity and is regulated by many of the oncogenic melanoma pathways. At the top of the figure selected therapeutic agents that target each of these genetic networks are shown [25].

2.4 Fibroblast growth factors (FGF) and FGF-receptors

2.4.1 Evolution of the FGF and FGFR gene family

Fibroblast growth factors (FGFs) make up a large family of polypeptide growth factors. The FGF Family comprises a signalling system that is conserved throughout metazoan evolution. During evolution, the FGF family expanded in two phases, during early metazoan evolution and during the evolution of early vertebrates. In the first phase, FGFs expanded from two or three to six genes by gene duplication, while in the second phase the expansion took place by two large genome duplications. In contrast, the FGFR family has expanded only in the second phase. However, the acquisition of alternative splicing by FGFR has increased their functional diversity. The mechanisms that regulate alternative splicing have been conserved during evolution [26, 27, 28].

In the mammalian FGF family, there are 22 genes encoding for FGFs. The human FGF gene family can be divided into seven subfamilies based on structural homologies and phylogeny: The intracellular subfamily = FGF11 subfamily: FGF (11-14), the hormone-like subfamily: FGF19, FGF21 and FGF23 and the canonical subfamilies, which can be divided into five groups: the FGF1 group (FGF1, FGF2), FGF4 group (FGF4-6), FGF7 group (FGF3, FGF7, FGF10, FGF22), FGF8 group (FGF8, FGF17, FGF18) and FGF9 group (FGF9, FGF16, FGF20) (Figure 5).

Members of these subfamilies share a varying degree of sequence, biochemical and developmental similarities [26, 28, 29]. FGF-like peptides (11-14) do not activate the FGF-dependent signaling pathway and therefore are not considered to be members of the genuine FGF family although they share a high sequence identity with this family [30].

FGF receptors are a subfamily of receptor tyrosine kinases (RTK). Four genes encode the four known FGF receptors. Each of these genes is localized on different chromosome and alternative splicing causes functional diversity and specify of FGFRs (Figure 5) [31, 32, 33].

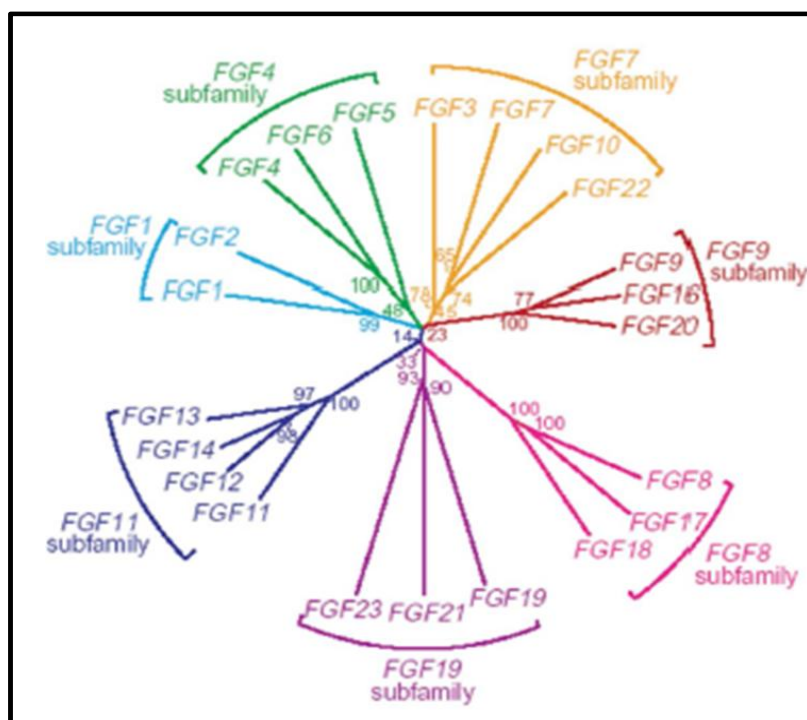


Figure 5: Members of the human fibroblast growth factor (FGF) gene family [34].

FGFR1	8p12	FGFR1b FGFR1c	FGF1,2,3 and 10 FGF1,2,4,5 and 6
FGFR2	10q26.12	FGFR2b FGFR2c	FGF1,3,7 and 10 FGF1,2,4,6 and 9
FGFR3	4p 16.3	FGFR3b FGFR3c	FGF1 and 9 FGF1,2,4,8 and 9
FGFR4	5q35.2	FGFR4	FGF1,2,4,6,8 and 9

Table 1: FGF-Receptor genes, their chromosomal localizations, splice variants and ligand Specificities for FGF1-FGF10 are shown [34].

2.4.2 Structural and functional properties of FGFs and FGF-receptors

Human FGF family members range in size from 17 kDa to 34 kDa and possess a homologous 120 amino-acid central core domain with twelve anti-parallel β -strands in core domain [35, 36]. Most FGFs (3, 4, 5, 6, 7, 8, 10, 15, 17, 18, 19, 21, 22, 23) have classical amino terminal signal peptides that ensure the secretion through the endoplasmic reticulum pathway.

In contrast FGF 9, 16 and 20 are secreted in spite of their lack of a signal peptide, whereas, FGF1 and 2 seem to remain intracellular until they are released from

decaying cells. FGFs 11-14 also lack a signal sequence and are considered remaining intracellular and functioning within cells in a receptor independent manner [27, 29]. FGF signalling exerts a combination of biological and physiological effects (Table 2) that contribute to chemotaxis, cell growth, proliferation and differentiation and induced mitogenic and angiogenic activity in cells of mesodermal and neuroectodermal origin [37].

Specific members of the FGF family are key molecules during embryogenesis [38, 39]. They also play crucial roles in development and wound healing. Several FGFs play an essential role during gastrulation, the formation of all three germ layers and organogenesis especially in lung, limb and the nervous system [29, 40, 41, 42]. For instance, fibroblast growth factor 5 (FGF5) is widely expressed in embryonic but scarcely in adult tissues [43]. FGF5 was originally identified based on a screening approach for genes present in tumors that are able to transform NIH 3T3 cells [44]. The FGF5 protein is 267 amino acids long and possesses 40% and 50% homology in the core region to FGF1 and 2 and is secreted as a glycoprotein [44, 45, 46].

Human and murine FGF5 genes contain consensus sequences for secretion and their translation is stringently controlled by several upstream AUGs [46]. It is suggested that FGF5 plays a role in embryonic stem cell regulation especially for the neuroectoderm [47, 48]. FGF5 is expressed in neonatal brain, therefore it is tempting to suggest that FGF5 is a neurotrophic factor [49]. FGF5 plays a role in the peripheral nervous system as a muscle-derived trophic factor for motoneurons [50]. FGF5 negatively regulates a step of the hair follicle growth cycle. FGF5 knockout mice exhibit abnormally long hair in the absence of any other defect and loss-of-function mutations in the FGF5 gene account for hereditary variations in hair length in canines and felines [30].

The role of FGFs in organogenesis has been shown in mouse genetic models as well as human pathologies. Examples are FGF8 knockout mice that are defected in gastrulation and FGF9 and FGF10 knock mice which die at birth because they have not developed functional lungs [28]. FGFs can also stimulate wound healing angiogenesis and tissue repair in adult organism.

Regarding to wound healing, FGF1, FGF2 and epithelial specific FGFs 7 and 10 stimulate proliferation and cell migration in the mesenchyme and the epithelium to achieve wound closure and re-epithelialization [52]. Endothelial cells express the IIIc-forms of FGFR2 and FGFR3 which make them responsive to FGFs that are

involved in wound healing responses [28]. It has been shown that FGF2 can stimulate the sprouting of new vessels in response to neovascularisation [28]. In addition to FGF2, some other FGFs are involved in angiogenesis for example FGFs 16 and 18 in cardiac tissue [52]. In some cells, FGF-induced activation of FGFRs leads to proliferation, migration and differentiation in other cell types it contributes to cell cycle arrest, apoptosis or inhibition of differentiation [53].

Nr.	Fibroblast growth factor (FGF)	Phenotype of knockout mouse	Physiological role
1	FGF1	Normal	Not established
2	FGF2	Loss of vascular tone slight loss of cortical neurons	Not established
3	FGF3	Inner ear agenesis in humans	Inner ear development
4	FGF4	Embryonic lethal	Cardiac valve leaflet formation limb development
5	FGF5	Abnormally long hair	Hair growth cycle regulation
6	FGF6	Defective muscle regeneration	Myogenesis
7	FGF7	Matted hair reduced nephron branching in kidney	Branching morphogenesis
8	FGF8	Embryonic lethal	Brain, eye, ear limb development
9	FGF9	Postnatal death Gender reversal lung hypoplasia	Gonadal development organogenesis
10	FGF10	Failed limb and lung development	Branching morphogenesis
11	FGF16	Embryonic lethal	Heart development
12	FGF17	Abnormal brain development	Cerebral and Cerebellar development, Bone development
13	FGF18	Delayed long-bone ossification	
14	FGF19	Increased bile acid pool	Bile acid homeostasis Lipolysis Gall bladder filling
15	FGF20	No knockout model	Neurotrophic factor
16	FGF21	No knockout model	Fasting response Glucose homeostasis lipolysis and lipogenesis
17	FGF22	No knockout model	Presynaptic neural organizer
18	FGF23	Hyperphosphataemia Hypoglycaemia immature sexual organs	Phosphate homeostasis vitamin D homeostasis

Table 2: The physiology of FGFs [55].

2.4.3 FGF-receptors (FGFRs)

FGFRs belong to the class IV family of RTKs. Four different FGFRs are known. They possess similarities in their amino acid structure. The FGF receptors begin with an extracellular N-terminal signal peptide. The intracellular region includes

characteristic sequence containing the amino acid cysteine in a specific spacing. These cysteines are stabilized by disulfide bridges, which build the structure of the three Immunoglobulin-like domains (Ig I-III). In addition FGFRs contain a cluster of acidic amino acids between Ig I and Ig II forming a linker region called acidic box and a transmembrane domain followed by the tyrosine kinase domain in the intracellular region, which is subdivided into TRK1 and TRK2 (Figure6).

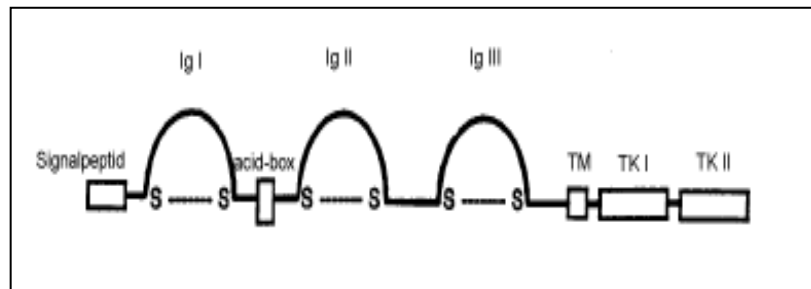


Figure 6: Structure of FGF receptors [56].

The FGF signaling pathway induces a variety of different effects. In order to achieve this amount of diversity the signaling system requires a variation at the level of the receptor. Different forms of receptors are generated through different expression of FGFR genes and alternative splicing of the same gene [55]. The Ig III-like domains of FGFR 1-3 contribute to different splicing by creation of IIIb and IIIc variants of the respective receptors (Figure 7).

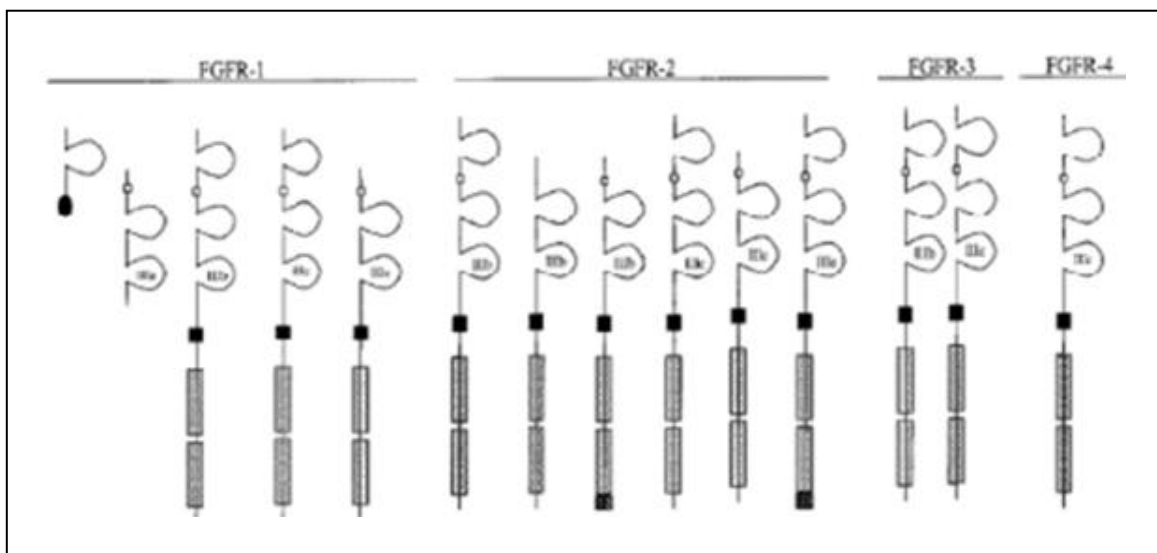


Figure 7: Overview of variants of FGF-septors generated by the mechanism of alternative splicing. Concerning the FGFR-2 gene, Ig domain IIIb is pre-dominantly expressed in the epithelial lineage, while Ig IIIc domains are only expressed in the mesenchymal lineage [55, 56, 57].

In general, the IIIb isoforms are expressed on epithelial cells, while the IIIc isoforms are often expressed on mesenchymal cells.

It is suggested that changes in the IgIII domain influence ligand binding (Figure 8). In addition specific heparin-binding sites in IgII domains of FGFRs are required for a strong binding to heparansulfateproteoglycans (HSPG). It was shown that the binding of fibroblast growth factors to these extracellular polysaccharides constitutes a mechanism limiting the diffusion radius of FGFs and sequestering them in the extracellular matrix of the connective tissue. FGFs can be released from such microenvironmental stores by proteolytic enzymes or by the action of a specific FGF-binding protein (FGF-BP). This protein is secreted into the extracellular space where it reduces affinity of the FGFs to heparin to make it available for signalling. This was shown for FGFs1 and 2 during wound healing [28].

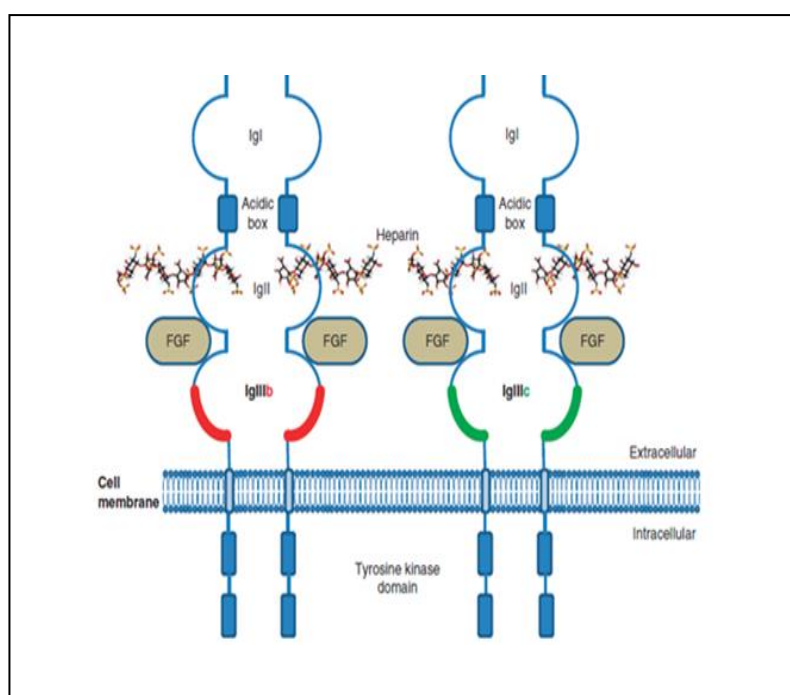


Figure 8: Protein structure of FGFRs. FGFRs is receptor tyrosine kinases consisting of cytoplasmic interrupted kinase domains and transmembrane domains with high degrees of homology between different FGFRs. The extracellular domains consist of three immunoglobulin (Ig)-like loops that bind FGFs between Ig-loop 2 and 3. FGFRs 1-3 are subject to alternative splicing events that affect Ig-loop 3 and therefore have large effects on the receptors ligand specificity. HSPGs mediate receptor-ligand binding [28].

2.4.4 Dysregulation of FGF signaling in cancer

The binding of FGFs to their receptors induces RTK dimerization, which undergo auto/trans-phosphorylation on tyrosine residues located within the carboxy terminal cytoplasmic tail. These phosphorylated residues serve as a docking site for downstream signaling proteins.

Two main pathways are involved in downstream signaling. Signaling through binding of FGF-receptor substrate FRS2 α to the juxtamembrane region of the receptors via a Src-homology 2 (SH2) domain leads to activation of the ras-pathway and further downstream the PI3K/Akt-pathway and/or MAPK pathway. The second pathway recruits phospholipase C γ to produce 1, 2-diglycerides to activate PKC that synergistically upregulates MAPK signaling [31, 58].

Activation of various signal transduction cascades plays a significant role in pathogenesis of human cancers via stimulation of tumor growth/survival and neoangiogenesis and tumor cell migration (Figure 9).

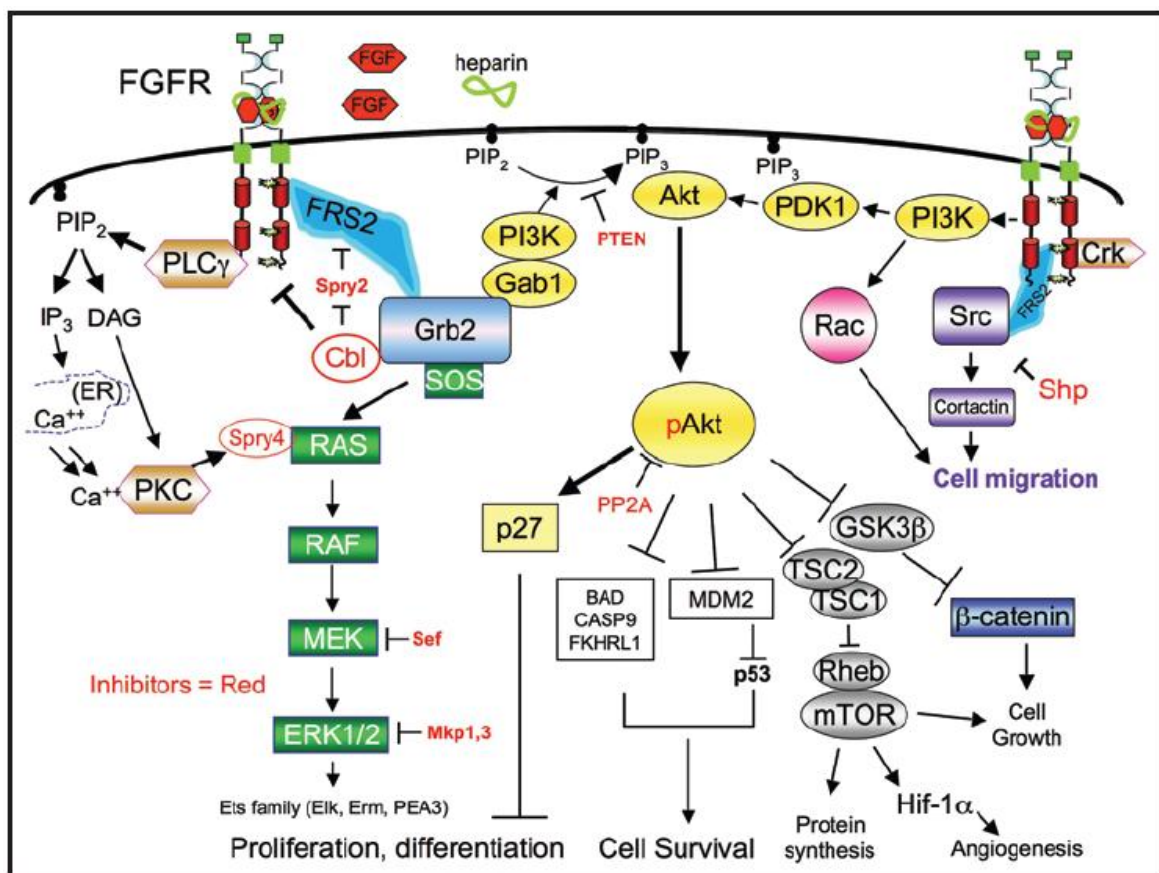


Figure 9: Overview of oncogenic signal cascades activated by FGFs [59].

There are many possibilities that can cause to dysregulation of FGF signaling pathways. Over- expression of FGF ligands has been observed in a great variety of human tumors. Autocrine production of FGFs is a common hallmark of cancer and over-expression of secreted FGFs supports autocrine signaling loops. Up-regulation of FGF2 is found in breast and lung cancer. In addition over- expression of FGF3, 4 and 8 which are normally not expressed to high levels in adult tissues has been

found in a number of human neoplasms, for instance in Kaposi's sarcoma, and in carcinomas of the breast, prostate, ovary and esophagus [60-63]. Over-expression of FGF18 and FGF19, which act through the receptors FGFR3-IIIc and FGFR4 on the tumor cells, has been shown in colon cancer.

Dysregulation of FGF signaling can also occur by alteration of FGFRs through activating mutations, amplifications and translocations of FGF receptor genes. Mutations in FGFR genes are found not only in the kinase domain but also over the complete length of the gene [28]. FGFR2 mutations are mainly observed in epithelial tumors, while FGFR3 mutations are common in multiple myeloma and autosomal mutations in FGFR4 are frequent in rhabdomyosarcoma [64, 65].

Concerning FGFR1 and FGFR2, deregulations are more commonly by gene amplification. FGFR1 amplification has been described for example in breast cancer, ovarian cancer, bladder cancer, oral squamous cell carcinoma and rhabdomyosarcoma. FGFR3 over-expression in multiple myeloma is achieved by translocations. These translocations are involved in conversion to full multiple myeloma [66].

Regarding tumor cell migration, there are many studies, which suggest that FGFs stimulated the tumor cell migration and may be a drivers of metastasis. In many tumor types FGFs induced activation of alternative survival pathways and provide a strong growth advantage for the tumor through autocrine FGFs and/or constitutively activated receptors [28]. In addition to autocrine stimulation, FGFs 1, 2, 4, 5, 8 and 18 have paracrine effects on vascular endothelial cells through FGFRs 1 and 2 and induced endothelial cell proliferation and secretion of essential factor for angiogenesis like metalloproteases and plasminogen [67].

It is suggested that FGF5 may participate in autocrine and paracrine pathways promoting pancreatic cancer cell growth *in vivo* [68] and FGF5 was identified as an overexpressed antigen in multiple human adenocarcinomas [69]. The predominant FGF5-binding FGFR1 variant IIIc [70] was found to be up-regulated in various cancer types [71], thus generating the conditions for autocrine loops.

In astrocytic brain tumours oncogenic activities of FGF5 on growth- survival- and migration of tumor cells was shown [43]. In melanoma, an oncogenic role of basic FGF (FGF2) has been identified as an important hallmark of melanoma cells in contrast to normal melanocytes [72]. Compared to FGFR2 and 3, FGFR1 and FGFR4 are highly expressed in nearly all melanoma cell lines. Reports have

established a correlation between FGFR4 protein expression and survival of melanoma patients. In addition to FGF2, expression of FGF5 is also found in melanoma. Our previous data showed very low expression of FGF5 in melanocytes but over-expression of FGF5 in the majority of the tested melanoma cell lines [73].

3 Materials and Methods

3.1 Cell lines and media

The institute of Cancer Research supplied all melanoma cell lines (Table3), which have been described previously [74]. We used Roswell Park Memorial Institute (RPMI) medium with 10% fetal bovine serum (FBS) for all cell lines. RPMI medium is a hydrogen-carbonate buffer system in a solution of glucose, salts, amino acids and vitamins, which was purchased from Sigma Aldrich and uses phenol-red for indicating the pH-value. FBS (Sigma Aldrich) is used to supply cells with a variety of growth factors, hormones and trace elements to make cell survival in culture possible. Penicillin/streptomycin solution was added to the medium only during selection of stable transfectants, was bought from PAA and used at an end-concentration of 1%.

Cell line	Origin	Histology
VM-1 FTSL-A	LN	SMM
VM-21 RHTP	PT	NM
VM-7 GTBS	PT	NM
VM-8 GUBSA	LN	NM
VM-24 SHTJ	LN	Unknown
VM-48 KAKA	BR	NM
VM-47 HOST	BR	NM

Table 3: Used cell lines, including VM (Vienna Melanoma) numbers, origin and histology. Establishment of cell lines from primary tumours (PT), lymph node (LN) or brain (BR) metastases of malignant melanoma is also indicated.

3.2 Standard growth conditions

All melanoma cell lines were kept in a humidified incubator (Forma Scientific) at 37°C and 5% CO₂. Tissue culture flasks (T25 (=25cm²), T75 (=75cm²) and T175 (=175cm²)) were bought from Greiner Bio-One or from BD Falcon. 6-/12- and 24-well plates were bought from IWAKI, 96 well-plates from TPP. Medium with 10% FBS was always used for cells except where indicated otherwise.

3.3 Splitting

The medium was aspirated and cells were washed once with PBS (2.7 mM EDTA (Merck), 137 mM NaCl (Merck) and 10 mM Na₂HPO₄ (Merck), pH 7.4) Trypsin/EDTA (T/E, 0.01% EDTA (Fluka), 0.1% Trypsin (Difco)) was added onto the cell layer and incubated about 5 minutes at 37°C. Detachment was monitored using the

microscope. Cells were resuspended in medium and the desired number of cells was transferred into a new flask, containing fresh medium.

3.4 Cell counting

For cell counting, either a Casy Cell Counter (Schärfe) or a Neubauer Chamber were used [75].

3.5 Freezing

After culturing the cells to about 80% confluence, cells were trypsinized and resuspended in 5 ml medium and transferred to 15 ml Falcon tubes, pelleted at 600-800 rpm for 5 min. and supernatant was discarded. Cells were resuspended in 2 ml medium. If cells were on selection (for stable transfectants), the medium also contained the corresponding selection reagent as well as penicillin and streptomycin. DMSO (dimethyl sulfoxide) was added to a final concentration of 50 µg/ml and 1 ml of cell suspension was transferred into cryotubes (Greiner). The suspension was put on ice and cooled down in a styrofoam container at -80°C for at least 24 hours, but not longer than 72 hours. Afterwards, cells were transferred into a liquid nitrogen tank for long term storage.

3.6 Isolation of RNA

Medium was discarded, Trizol (Invitrogen) was added onto the cell layer and cells were incubated in Trizol solution for about 5 minutes. Lysates were transferred into 2 ml Eppendorf tubes. Chloroform (0.2 x vol. Trizol) was added, the tubes were vortexed and centrifuged at 12000 g for 15 min at 4°C. Aqueous supernatant, containing solubilized RNA, was transferred into new Eppendorf tubes and isopropanol (0.5 times vol. Trizol) was added and tubes were incubated for 10 min. and centrifuged again at 13000 g at 4°C for 11 min. Supernatant was discarded and 75% EtOH/DEPC (diethylpyrocarbonate-treated) was added onto the pellet and centrifuged at 13000 g at 4°C for 10 min. The alcohol was discarded and the pellet was air dried and resuspended in 15 µl DEPC water. Isolated RNA was stored at -20°C for shorter or at -80°C for longer periods of time.

3.7 Determination of RNA concentration

Determination of RNA concentration was achieved by OD₂₆₀ measurement on a NanoDrop 1000 spectrophotometer (Thermo Fisher Scientific).

3.8 Synthesis of cDNA

2 µg RNA were diluted with DEPC water to 13 µl and incubated for denaturation at 70°C for 10min. Tubes were put on ice and 7 µl cDNA Synthesis Master Mix (MM) were added to a total volume of 20 µl. The reaction was incubated for 1.5 hours at 37°C. The quality of cDNA was tested by performing standard RT-PCR of a “housekeeping gene” followed by agarose gel electrophoresis. cDNA was stored at – 20°C.

	Solution (Concentration)	Volume (µl)
cDNA Synthesis Master Mix (1 x)	M-MLV RT buffer (5 x; Promega)	4
	Hexanucleotides (20 ng/µl)	0.5
	dNTPs (10 mM)	1
	DTT (100 mM)	1
	MMLV-RT (200 u/µl; Promega)	0.5
		7 µl total volume

3.9 TaqMan - “Real Time” quantitative RT-PCR (qRT-PCR)

TaqMan Master Mix was prepared on ice and 2 µl cDNA were added into two wells (per sample) of an Optical 96-Well Reaction Plate (Micro AmpR; Applied Biosystems). Master Mix was added to a total volume of 12 µl and mixed. PCR was started and fluorescence measurement occurred after each cycle using an ABI Prism 7000 SDS thermocycler (ABI), according to ABI manuals. Taqman probes which were used in this thesis are listed below.

	Solution (Concentration)	Volume (µl)
TaqMan qRT-PCR Master Mix (1 x)	TaqMan Probes (Applied Biosystems)	1.25
	TaqMan Master Mix (Applied Biosystems)	12.5
	water bidest.	9.25
cDNA		2
		23 total volum

Taqman-Probes used for FGF5

HS 00170454m L
Lot :657375

House-keeping gene

Beta 2-microglobulin (B2M)

3.10 Gel electrophoresis (Nucleic acids)

Agarose gels consisting of 1% (w/v) agarose (Biozyme) in 0.5 x TBE buffer (5.4 g/L Tris (Fluka) 2.75 g/L boric acid (Sigma), 1 mM EDTA), were used for size separation of DNA fragments of 1-3 kilobases (kb). 6 x loading buffer (333 µL/mL 6 x loading dye (Fermentas), 250 µL/mL 80% glycerol (Merck), 66.5 µL/mL 0.5 M EDTA, 0.5 µL/mL 10 000 x Vistra-Green (GE Healthcare) was added to samples and loaded on to the gel. 2 µL Gene Ruler 1 kb DNA Ladder (Fermentas) mixed with appropriate amounts of water and loading buffer were used as a marker. Gel was run at a voltage of 50 V for 10 min, followed by 90 V for 30 min (power supply: Bio-Rad), in 0.5 x TBE as a running buffer. 2% gels (marker: GeneRuler 100 bp Plus DNA ladder (Fermentas)) were used for smaller fragments and 0.5% gels for larger fragments. Bands were visualized using a FluorImager 595 Scanner from Molecular Dynamics.

3.11 Isolation of proteins

Lysis buffer II (LBII) was used for isolation of all non-secreted proteins for Western-blot and SDS-PAGE analysis. Cells were trypsinized and washed with cold PBS. Centrifugation was done at 800 rpm for 5 minutes. All successive steps were done on ice. LBII was added onto the cell pellet. Volume of lysis buffer depended on cell amount and usually ranged between 30 µl for around 500 000 cells and 120 µl for 2 million. The pellet was resuspended by pipetting up and down for several times, then the Insoluble components were removed by centrifugation at 4°C and 20 800 g for 10 minutes. Aqueous supernatant was transferred and stored at -20°C, for longer periods at -80°C.

3.12 Determination of protein concentration

The protein concentration of samples was determined by the Bradford Protein Assay (1:5 dilution in dH₂O, Biorad) in duplicates. Samples, as well as BSA bovine serum albumin as standard protein for the calibration curve (Table 4 and Figure 10) were placed into PS microplate 96-well (Greiner). 190 µl of diluted Bradford solution was added and mixed, then incubated for about 10 minutes at RT. Absorbance was measured at 562 nm by using a SynergyHT plate reader (BioTEK) and Gen5 software (BioTEK). From the calibration curve the concentration of samples was calculated. Obtained concentrations had to be multiplied by 10, because of the 1:10 dilution of the samples.

	Water (μl)	Lysis-Buffer (μl)	BSA (1 μg / μl)	Conc.(μg / μl)	Sample (μl)
blank	9	1	0	0	
1	8	1	1	0,1	
2	7	1	2	0,2	
3	5	1	4	0,4	
4	3	1	6	0,6	
	1	1	8	0,8	
	0		9	0,9	
	9				1

Table 4: Pipetting Scheme of BSA standards and protein samples. All concentrations were calculated by taking the average of double determinations.

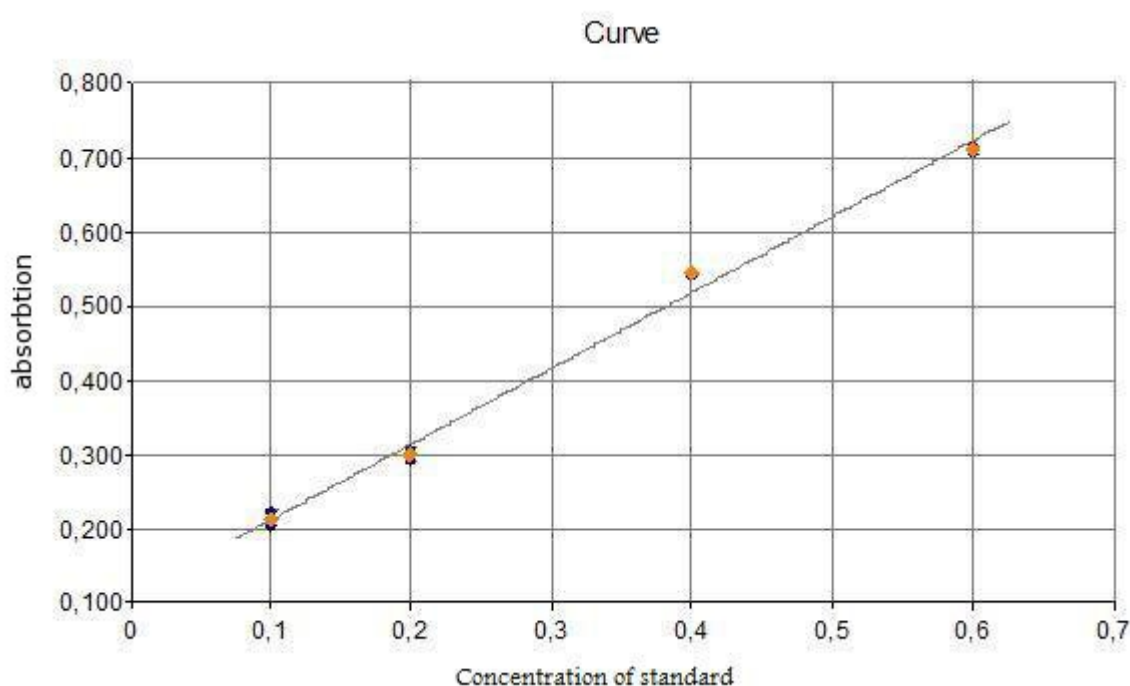


Figure 10: Example of calibration curve used for determination of protein concentration by Bradford Assay.

3.13 SDS-polyacrylamid gel electrophoresis

For detection of a protein of interest in cell lysate or supernatant, samples were subjected to SDS-PAGE [76] and Western blot [77]. The Mini Protean 3 system (Bio-Rad) was used for gel electrophoresis and transfer of protein to a PVDF membrane (Hybond-P, GE Healthcare) for immunodetection. Separating and stacking gel were prepared as described in (Table 5) with densities between 7.5 and 15% according to protein sizes desired to be investigated. The separation gel was cast and topped with isopropanol. After polymerization, the isopropanol layer was rinsed off with filter paper (Schleicher and Schuell). Afterwards, the stacking gel was cast on top and sealed with a ridge. Following polymerization, the ridge was removed and pockets were cleaned with SDS Running Buffer (25 mM Tris, 192 mM glycine and 0.1% SDS),

which was also used as running buffer for SDS-PAGE. 40 µg proteins of samples were prepared using 5 x Laemmli loading buffer. Samples were heated for 5 minutes at 95°C to denature proteins and loaded onto the polyacrylamide gel. The PageRuler™ Prestained Protein Ladder (Fermentas) was used to determine the molecular weight of the proteins loaded. Protein samples were assimilated at 50 V in the stacking gel and separated at 120 V in the separating gel.

Separation Gels	10%	Volume	Stacking Gel	4%	Volume
Water	1.960	ml	Water	1.5	ml
1.6 M Tris pH 8.8	1.250	ml	1.6 M Tris pH 8.8	0.625	ml
20% SDS	50	µl	20% SDS	12	µl
30% Acrylamid/Bis; 29:1(Bio-Rad)	1.675	ml	30% Acrylamid/Bis; 29:1(Bio-Rad)	0.325	ml
10% APS (Merck)	25	µl	10% APS (Merck)	25	µl
TEMED (Amresco)	5	µl	TEMED (Amresco)	2.5	µl

Table 5: Recipes for PAGE gels

3.14 Western blot

The Western blot is a standard method for detection of specific proteins. After protein separation via SDS-PAGE, Proteins were transferred to a polyvinylidene fluoride (PVDF) membrane. The Mini Protean 3 system was used for blotting. Sandwiches of buffer soaked sponges and filter papers were prepared carrying the positively charged membrane (activated with methanol) and the gel. The blotting sandwich was assembled, and transfer was performed at a voltage of 18 V, overnight in the fridge (4°C). After protein transfer, the membrane was dried and reactivated with methanol. Quality of transfer was controlled by staining protein bands with Ponceau S Solution (0.5 g/l Ponceau S (Sigma) and 1 ml/l glacial acetic acid [79]. Membrane was incubated in the staining solution for about 5-20 minutes. The background was removed by washing with distilled water on the shaker. To increase quality, water was changed several times. Afterwards, the staining was documented using a photocopier. After reactivating with methanol and washing with PBST or TBST, the membrane was blocked for 1 hour with 5% Skim Milk Powder (Fluka) at RT on the shaker. Blocking solution was washed off 3 x 10 minutes with TBST. Incubation with primary antibodies (Table 6) occurred over night at 4°C on a rotator in a 4°C room. Next day, after 3 washing steps of 15 minutes each with PBST/TBST, the membrane was incubated for 1 hour with secondary antibodies.

PVDF membrane was washed again, 3 x with TBST and 2 x with TBS, then incubated upside down on a parafilm with Immune-Star WesternC reagent (Bio-Rad) and visualized using Hyperfilm ECL (GE Healthcare).

Primary Antibodies	Dilution	Supplier	Dilution	Size of Target
FGF5 poly clonale goat	1:1000	Santa Cruz sc124	BSA	30 KDA

Secondary Antibody	Dilution	supplier	Dilution	Size of Target
Anti goat - HRP	1:10 000	Dako	M	n/a

Table 6: List of antibodies used for immunodetection. Concentration of BSA as diluent was 3%, but for milk powder (M) was 5%.

3.15 Lipofection

3×10^5 cells were seeded with 2 ml 10% RPMI medium into 6-well plates and incubated overnight. Next day, cells were adherent and around 50-80% confluent. FuGENE 6 (from Roche) was used as lipofection reagent. 3 μ l transfection reagent were added to 97 μ l serum-free medium (SFM; RPMI without FBS) mixed and incubated 5 minutes. 1 μ g plasmid was added and incubated for another 25 minutes. Transfection suspension was added dropwise onto the medium-containing dishes with the cells and gently mixed. The following day, a change of medium was performed.

3.16 Selection of stable transfectants

In order to select for cells which have integrated the plasmids coding for FGF5 or short hairpin (sh)RNAs and a selection marker into their genome, the antibiotics neomycin / G418 and puromycin were used (Figure 11, Table 7).

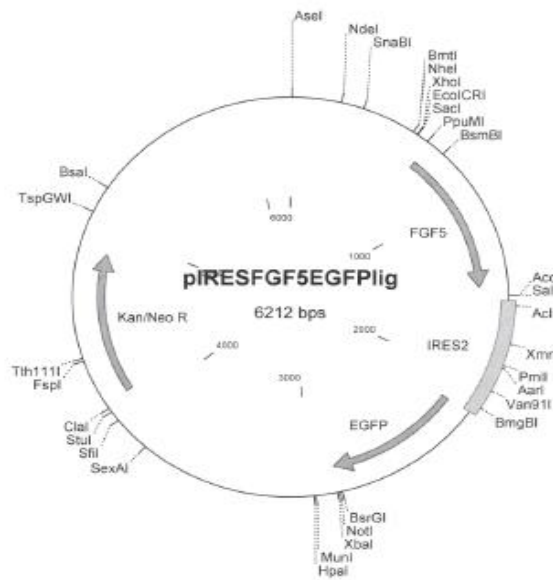


Figure 11: PIRESEGF5EGFP lig vector containing the FGF5 cDNA.

To reduce the risk of fake clone formation, a plasmid encoding for a bicistronic mRNA containing the gene of interest and GFP, separated by an internal ribosome entry site IRES [78] was used. Western blot analysis and qRT-PCR were performed to assess the expression of FGF5.

To ensure good growth conditions, the selective medium was changed every two to three days. Usually after 1-2 weeks small, G418-resistant, GFP-fluorescing clones appeared. They were left to grow fully confluent for further sorting with FACS for GFP-positive cells.

Cell line	G418 PAA ($\mu\text{g/ml}$)
VM 1	200
VM 21	150

Table 7: End-concentration of additives during selection and cultivation

3.17 FACS sorting of GFP-positive stable clones

The day before sorting, 5 l filter-sterilized 1 x PBS, 2 l filter-sterilized 70% ethanol and 2 l filter-sterilized distilled water were prepared. 50 ml Falcon tubes containing 35 ml growth medium containing 10% FBS were incubated over night at 4°C. Before sorting, the cells were trypsinized, pelleted and washed one time with PBS. Afterwards the pellet was resuspended in 1ml serum-free medium containing

penicillin/streptomycin. The growth medium in the 50 ml Falcon tube was removed and instead 5 ml medium containing penicillin/streptomycin were added in each of the prepared tubes. As negative controls untransfected cells were prepared. FACS tubes containing the cells and Falcon tubes containing the growth medium were stored on ice and FACS analysis was performed. An appropriate number of GFP-positive cells were sorted and centrifuged at 800 rpm (Beckman CS-6KR Centrifuge) for 5 min. The hardly observable pellet was resuspended in growth medium containing penicillin/streptomycin and G418 and transferred to a fresh culture dish.

3.18 Lentiviral transduction

1.6×10^4 cells (GUBSA, GTBS and HOST) were seeded in a 96 –well plate and incubated overnight. Next day medium was replaced with 110 μ l fresh medium containing hexadimethrine bromide (final concentration 8 μ g /ml) and 5 μ l of lentiviral particles were added per well. Five different lentiviral particles each expressing a shRNA for silencing of FGF5 and a scrambled shRNA as control were used. After 24 h the medium containing the lentiviral particles was removed from the wells, and 120 μ l fresh medium were added to each well. Next day the medium was changed again to fresh medium containing the appropriate amount of puromycin (0.6 μ g/ml for VM 7 and VM 8 cells and 0.8 μ g/ml for VM 47 cells). Selective medium was changed every 3-4 days until no more cells died. Then cells were expanded to assay them for knock-down of FGF5.

Used Lentiviral particles

NM-004464	TRCN0000058878	1.9×10^7 TU
	TRCN0000058879	1.8×10^7 TU
	TRCN0000058880	2.1×10^7 TU
	TRCN0000058881	2.2×10^7 TU
	TRCN0000058882	1.9×10^7 TU
Scrambled		

3.19 Cell viability assay (MTT assay)

The MTT assay is a colorimetric assay that utilizes MTT (3-[4, 5-dimethylthiazol-2-yl]-2,5- biphenyl tetrazolium bromide) to assess cell viability. MTT is a water-soluble yellow dye that is readily taken up by viable cells. Cell lines (10^3 cells per 96-well) were seeded in 100 μ l medium with 10% FBS and after 24 h inhibitory or stimulatory

molecules were added as 2 x concentrations in 100 µl serum-free medium, resulting in a total volume of 200 µl (5% FBS). 5 days after treatment, cells were incubated for 1-2 hrs at 37°C with the EZ4U reagent (Biomedica) according to the manufacturer's instructions. To measure the cell viability, absorbance was measured at 450 nm, with 620 nm as reference wavelength.

3.20 Clonogenic assay

To test the capability of adherent cells to survive and to form colonies, cells were seeded in 6-well plates at very low densities (3000-5000) with 2 ml RPMI medium (10%). After about 7 days to two weeks colonies had formed, depending on the specific clonogenicity of the cell line used and these were stained with crystal violet.

3.21 Crystal violet staining

Supernatant was discarded; cells were washed in PBS and fixed by incubation in methanol:acetone (1:1) for about 20 minutes. Then cells were exposed to crystal violet solution (0.1g/ml crystal violet in absolute ethanol) diluted 1:1000 in PBS and incubated for another 20 minutes. Staining solution was discarded and dishes washed with aqua dest. Cells were air dried over night.

3.22 Growth curve

Melanoma cells were seeded in 6-well plates at a density of 1×10^5 cells per well in medium with 10% FBS. Cell number was determined every two days till day 8 with a Casy cell counter (Roche Innovatis AG, Bielefeld, Germany).

3.23 Invasion assay

To test the movement and invasion of cells, 12 well-plate formats were used. Porous membranes of transwell chambers were coated with 28 µl collagen and placed into the wells and incubated overnight at 4°C. 800 µl RPMI medium with 20% FBS were added into the well and 40000 cells in 200 µl 10% RPMI medium were seeded into the upper chamber resulting in a total volume of 1 ml. Migration through the membrane pores was visualized by crystal violet staining. Incubation time was 72 hours.

3.24 Soft agar assay

Preparation of soft agar medium and 1% agar solution was done the day before as follows: For preparation of soft agar medium, 2ml NaHCO₃ (110 mg/ml, in water

bidest.), 1 ml glutamine, 17 ml water (bidest.) and 50 µl folic acid were added to 10 ml (10 x) RPMI medium (Sigma). The solution was brought to a pH value of 8 and filter-sterilized. Then, 20 ml FBS and 1ml penicillin-streptomycin were added under sterile conditions. Considering the 1% agar solution, 1.2 g agar was added to 80 ml water (bidest.) and solubilised by boiling. Simultaneously another 30 ml of water (bidest.) were heated up and used to fill up the 80 ml suspension to 100 ml. At the end the suspension was boiled again. Afterwards, the solution was brought to a temperature of about 40°C for subsequent generation of the soft agar bottom. Soft agar medium and 1% agar solution were mixed 1:1. 1.5 ml was subsequently pipetted into each well of a six well plate, constituting the soft agar bottom. Air bubbles were prevented by leaving a low amount of solution in the pipette. Afterwards, plates were put in the fridge until the agar became solid, and then were put into the incubator over night.

Cells were trypsinized and the appropriate number of cells (10000) was centrifuged (800 rpm for 5 minutes) and the pellet was resuspended in 750 µl soft agar medium with a temperature of 37°C. 750 µl 1% agar solution (40- 41°C) were added to the cell suspension and mixed. A total volume of 1.5 ml was added on top of solid soft agar and resulted in a total volume of 3 ml (0.5% solid soft agar medium) per well of a six well plate. Solutions were kept on temperature in the water bath. To reduce velocity of temperature reduction, solutions were put into a tray containing warm water during pipetting. After the desired clone size was reached (>20 µm VM21, >15 µm VM 1), the number of clones above threshold level was determined under the microscope.

3.25 Hen´s egg test – chorionallantoic membrane (HET-CAM) assay

Preparation of eggs at breeding day 6: The eggs were disinfected by biotensid, the egg shell was opened with an electric drill. By drilling, the egg shell was removed taking care not to drill directly into the egg white to avoid contamination. 3 ml of albumin was extracted using a syringe with an 18 gauge needle. The hole was sealed with autoclaved aluminum foil and the eggs incubated further (37 ° C, 5% CO₂, 95% humidity). A filter paper was dipped into ether and put on the CAM. Subsequently, a sterile silicone ring with an internal diameter of 5 mm was placed on the sample area. Preparation of Cells: Melanoma cells with over-expression of FGF5 and mock controls were seeded into 75-cm² flasks and cultured to 70% confluence.

Then cells were trypsinized and 2×10^6 cells were counted and pipetted into Eppendorf tubes and centrifuged at 1200 rpm for 3 min. The supernatant was removed leaving only about 30 μ l. The cells were resuspended and applied to the surface of the CAM on the prepared sample area and incubated till breeding day 11. The growth of the cells and the changes in the CAM were observed daily by a stereo microscope and photographed using a camera.

3.26 Tumor growth in SCID mice

Cell lines were seeded in 10% RPMI and incubated over night. 1×10^6 cells per mouse in 50 μ l serum-free medium were injected subcutaneously into the flanks of SCID mice. Tumor formation was measured periodically by palpation, and the tumor size was determined using a Vernier calipe. Mice were sacrificed 40 days post injection. All experiments were carried out according to the Austrian and FELASA guidelines for animal care and protection. Tumors and organs were excised and tumor was divided into several parts. One part was immediately frozen in liquid nitrogen for extraction of RNA and protein and the second part was formalin fixed for paraffin embedding and histology.

3.27 Hematoxylin and eosin staining

Hematoxylin and eosin (H&E) stains are widely used for recognizing various tissue types and the morphologic changes that form the basis of contemporary cancer diagnosis. Hematoxylin has a deep blue-purple color and stains nucleic acids. Eosin is pink and stains proteins nonspecifically. In a typical tissue, nuclei are stained blue, whereas the cytoplasm and extracellular matrix have varying degrees of pink staining. Nuclei show varying cell-type- and cancer-type-specific patterns of condensation of heterochromatin (hematoxylin staining) that are diagnostically very important. Nucleoli stain with eosin. If abundant polyribosomes are present, the cytoplasm will have a distinct blue cast [79]. Paraffin embedded samples were deparaffinized in xylol and dehydrated in increasing percentages of ETOH. Slides were stained in hematoxylin (6 min) and counterstained in eosin (1min) following standards protocols.

3.28 Ki-67 immunohistochemistry

Determination of cell proliferation in tissue sections is often performed by detection of Ki-67 antigen. The polyclonal antibody (NCL-Ki67p) labels human Ki-67 antigen

during late G1, S, G2 and M stages of the cell cycle. Reagents: xylol, ethanol, PBS, citrate buffer, Tween 20 (for synthesis, Merck Best.Nr 8.22184.0500), ultra vision lp large volume detection system HRP polymer, normal goat serum and liquid DAB+ substrate chromogen system as well as hematoxylin, n-butylacetat, Entellan, Ki-67 (MIB-1) mouse monoclonale antibody at a 1:100 dilution (Dako) was used for the identification of murine Ki-67 antigen. All steps were performed following standard protocols.

3.29 Von Willebrand Factor (vWF) antibody staining

Von Willebrand Factor (vWF) is a large glycoprotein with a multimeric structure and a molecular mass ranging from 500 kDa up to more than 10,000 kDa. Expression of the von Willebrand Factor gene is tissue specific and confined to endothelial cells. Primary Antibody: Von Willebrand Factor, anti-human, rabbit polyclonal antibody at a 1:1000 dilution (Dako). All steps were performed following standard protocols.

3.30 Statistical analysis

Statistical analyses were performed with Graphpad Prism software. Student's t test was used for comparison of two groups and differences with p values < 0.05 were considered statistically significant.

4 Results

4.1 Expression analysis of fibroblast growth factor 5

Quantitative expression analysis of FGF5 (qRT-PCR) was performed in melanoma cell lines and primary melanocytes were included for comparison (Figure 12).

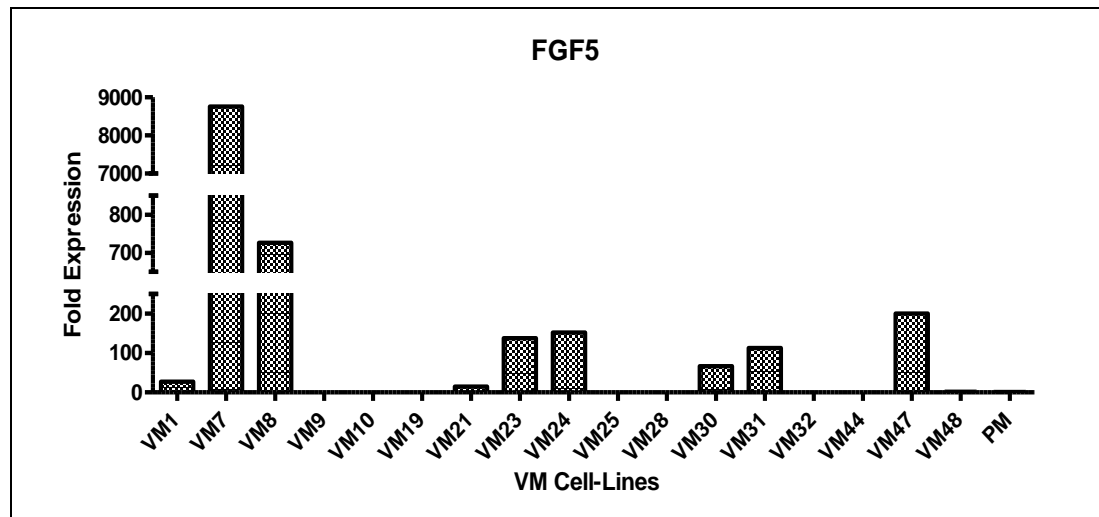


Figure 12: Quantitative expression analysis (qRT-PCR) of FGF5 in a panel of human melanoma cell lines (VM) compared to primary human melanocytes (PM). Strong over-expression (10-9000 fold) of FGF5 was seen in 9 of 17 melanoma cell lines [73].

Quantitative expression analysis revealed that FGF-5 was up-regulated in the majority of the tested melanoma cell lines.

4.2 Generation of isogenic cell models

Two melanoma cell lines VM1 (FTSL-A) and VM21 (RHTP) with low endogenous FGF5 expression were stably transfected with a vector expressing human FGF5 and green fluorescent protein (GFP) from a bicistronic mRNA as well as a G418 resistance marker. Cells were double selected for G418 resistance and GFP expression and the resulting cell pools were analyzed for FGF5 over-expression on mRNA and protein levels by qRT-PCR and Western blotting (Figure 13, 14). Mock transfected controls expressed only GFP and the antibiotic resistance marker. Transfectants achieved around 800-fold (VM1) and 600-fold (VM21) expression levels of FGF5 when compared to mock transfected controls. These high FGF5 expression levels correspond to those observed in melanoma cell lines with high endogenous FGF5 expression (Figure13). Western blot analysis of media supernatants from stable transfectants confirmed secretion of high amounts of FGF5 (Figure 14).

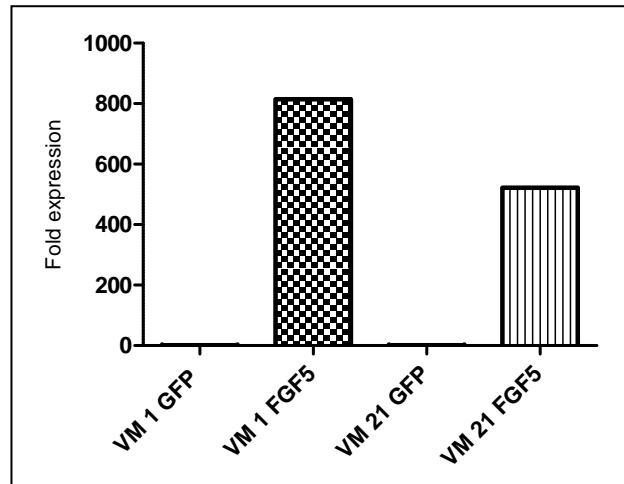


Figure 13: Quantitative expression analysis of FGF5 mRNA in VM1 and VM 21 cell lines, taking the respective GFP control as reference.

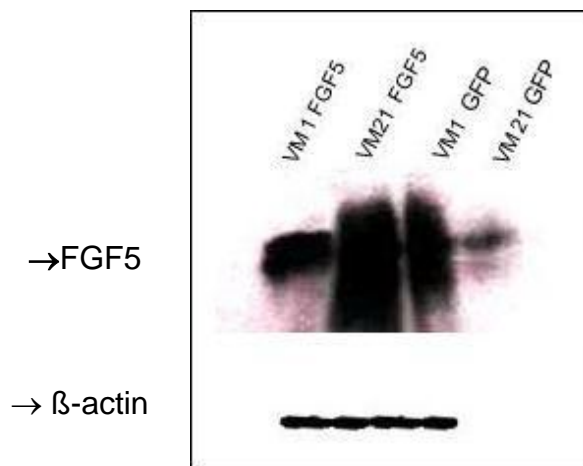


Figure 14: FGF5 protein expression was examined by western blot in the FGF5-transfected VM1 and VM21 cell line and GFP control cells. Specific FGF5 bands were detected at 30 kDa whereas β -actin bands were detected at 42 kDa.

4.3 Impact of FGF5 on the malignant phenotype of VM1 and VM21 *in vitro*

Cells with over-expressed FGF5 were compared to respective mock transfectants by subjecting them to different *in vitro* assays.

4.3.1 MTT assay

To check, whether FGF5 over-expression has any effect on cell viability, cell lines (VM1, VM21) were seeded in RPMI medium with 0.1% FBS or 10% FBS and grown for 5 days and the viability of cells was measured by MTT assay (Figure 15).

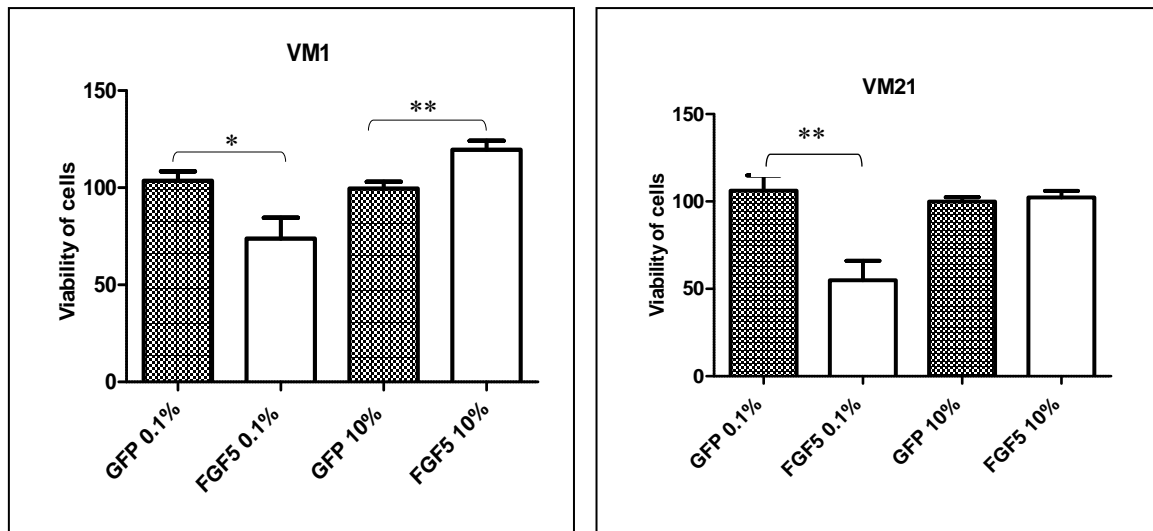


Figure 15: Viability of melanoma cell lines VM1 and VM21 with FGF5 over-expression incubated in RPMI medium with 0.1 or 10% FBS for 5 days. The GFP control was taken as reference. * $p < 0.05$, ** $p < 0.01$.

The viability of cells with FGF5 over-expression was decreased in RPMI medium with 0.1% FBS. In medium with 10% FBS there was either no difference (VM21) or a slight increase (VM1) in viability in the FGF5 overexpressing cells.

4.3.2 Growth curves

In a growth curve experiment, the effects of stable over-expression of FGF5, on the proliferation of melanoma cells were determined. Every two days cell number was measured by a Casy cell counter (Figure 16).

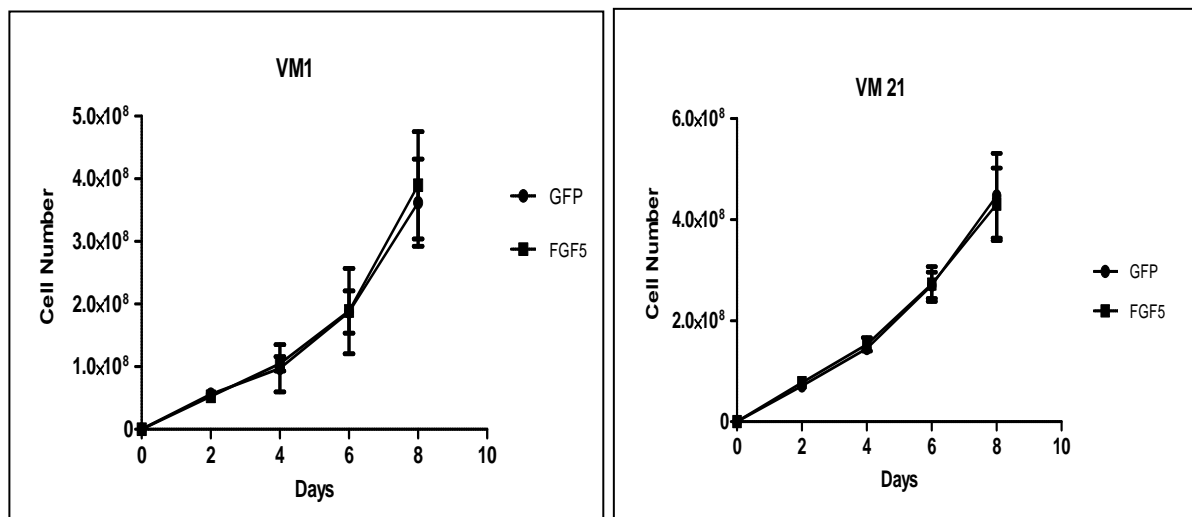


Figure 16: Proliferation of melanoma cell lines (VM1, VM21 expressing FGF5 determined by the Casy cell counter. 10 000 cells per 6-well were seeded.

Results showed no difference in proliferation of cells with FGF5 over-expression in contrast to GFP cells. Thus, FGF5 over-expression did not stimulate melanoma cell proliferation *in vitro*.

4.3.3 Clonogenic assay

Melanoma cells with over-expressed FGF5 were then tested for their ability to survive and form clones, when seeded at very low density. After desired clone sizes were reached, depending on the specific clonogenicity of the cell line, cells were fixed and stained with crystal violet (Figure 17).

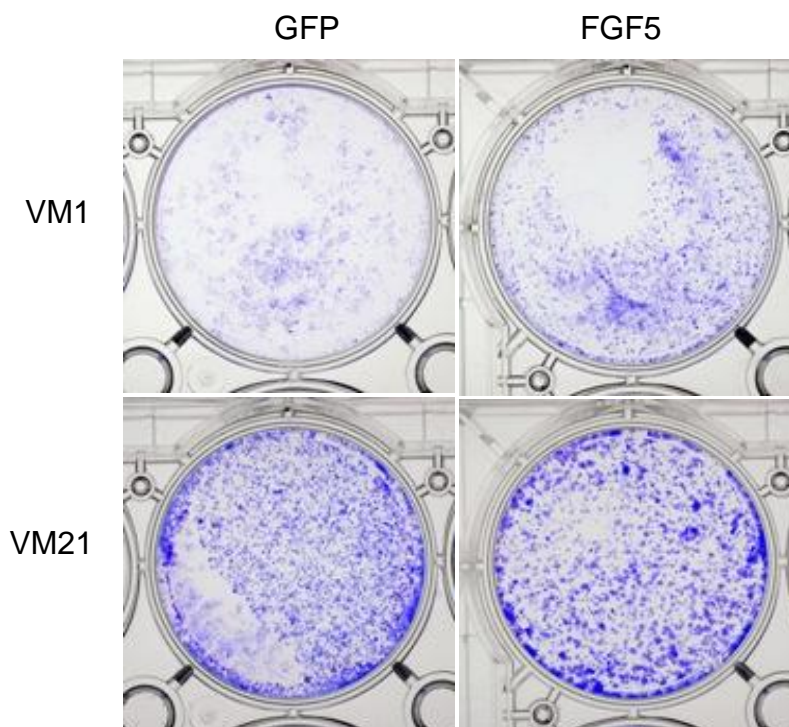


Figure 17: Examples of clonogenic assays of transfected VM1 and VM21 cell lines. Cells were seeded at low densities (5000 cells/6-well).

After staining the colonies with crystal violet, the dye was dissolved with 10% SDS solution and photometric measurement of the crystal violet absorption was performed. The amount of crystal violet which was taken up by the cells serves as a readout for the number of cells (Figure 18).

Because of the high mobility of VM1 cells, it was difficult to identify individual colonies in these cells. Results showed that in clonogenicity assays, colony formation was not significantly influenced by FGF5 in the VM21 cell line. According to photometric measurement of the crystal violet absorption, there is an increased clonogenicity in VM1 cells with FGF5 over-expression compared to GFP control cells.

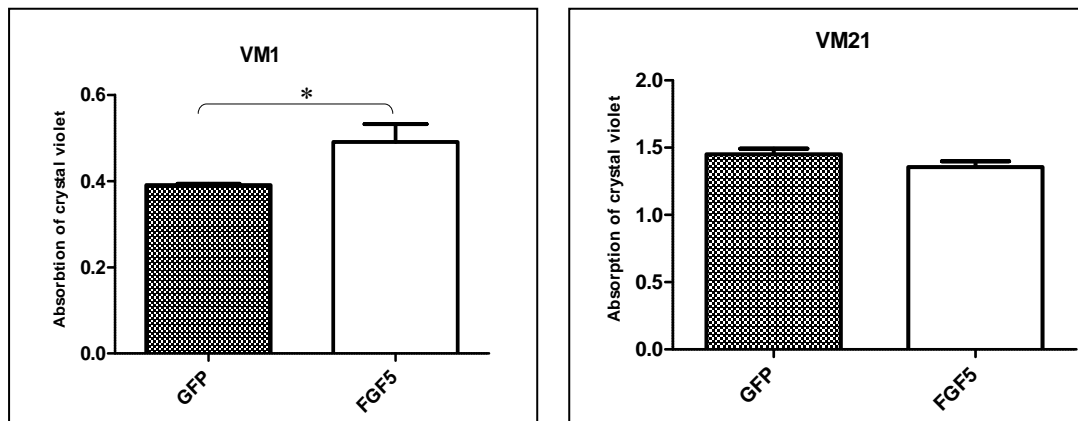


Figure 18: Photometric measurement of the crystal violet absorption in VM1 and VM21 cell lines showing a difference in clonogenicity of VM1 with over-expressed FGF5 compared to GFP. * $p < 0.05$ No difference was observed in colony formation of VM21 cells.

4.3.4 Soft agar assay

VM1 and VM21 cell lines were tested for their anchorage independent growth in three dimensional cultures. Cells were seeded in 10% RPMI medium including agar. Colony formation was monitored and the number of clones with a diameter above a specific threshold ($> 20 \mu\text{m}$ VM21, $> 15 \mu\text{m}$ VM1) was calculated. Cells were incubated about one month (Figure 19, 20).

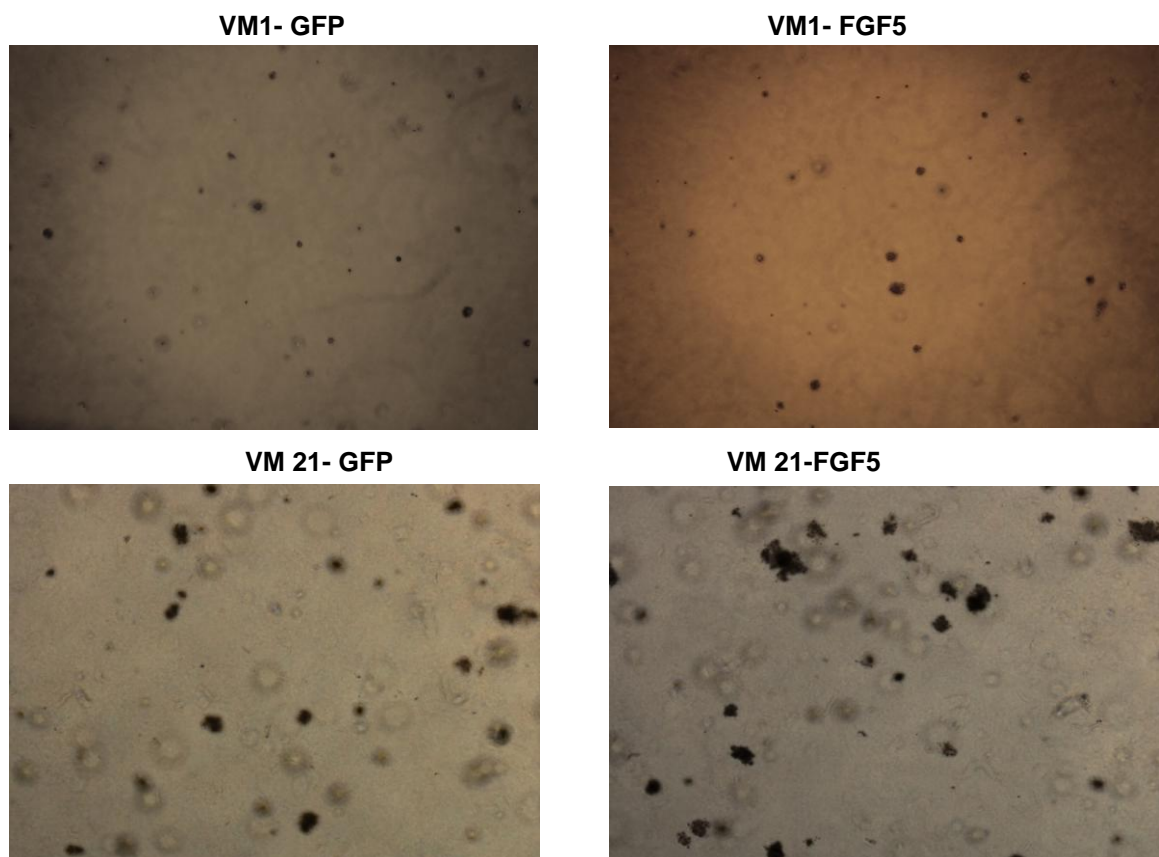


Figure 19: VM1 and VM21 cells with over-expressed FGF5 were plated in soft agar at a density of 10000 per 6-well. Clones formed under anchorage-independent conditions were evaluated after approx. 4 weeks of incubation.

Results showed no significant impact on the ability of cells expressing FGF5 to form clones in soft agar in contrast to cells with the GFP construct.

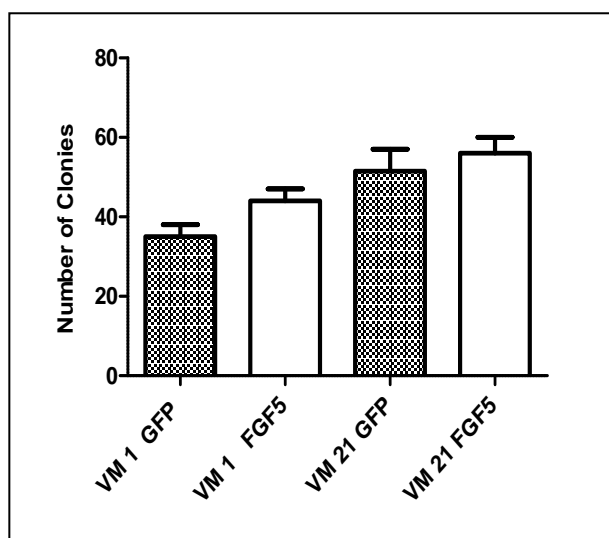


Figure 20: Results of soft agar assays. VM1 and VM21 cell lines were tested. 10 000 cells were seeded. Four different areas per well were counted.

4.3.5 Scratch assay

The scratch assay (wound healing assay), is an in vitro method to investigate the migratory ability of cells. In a monolayer of cells a scratch "wound", is made with a pipette tip, so that a cell-free gap forms. The adjacent cells can move into this vacant space. This is achieved through active cell movement. With this assay, the migration ability of VM1 and VM21 cells was tested after 4, 8, 24 and 48 h. Photographs after 4h are not shown (Figure 21, 22, 23, 24).

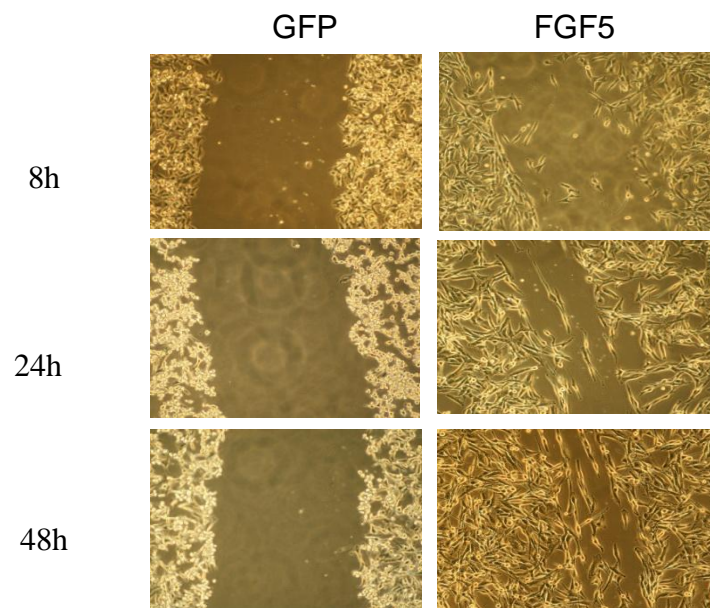


Figure 21: Example of a scratch assay of the VM1 cell line with over-expressed FGF5, after 8, 24 and 48h

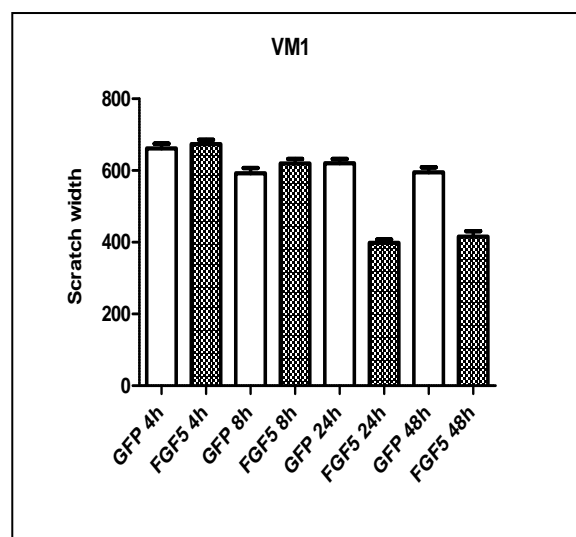


Figure 22: Results of relative Migration of VM1 cells expressing FGF5 after 4, 8, 24, 48h. GFP cells were taken as a control.

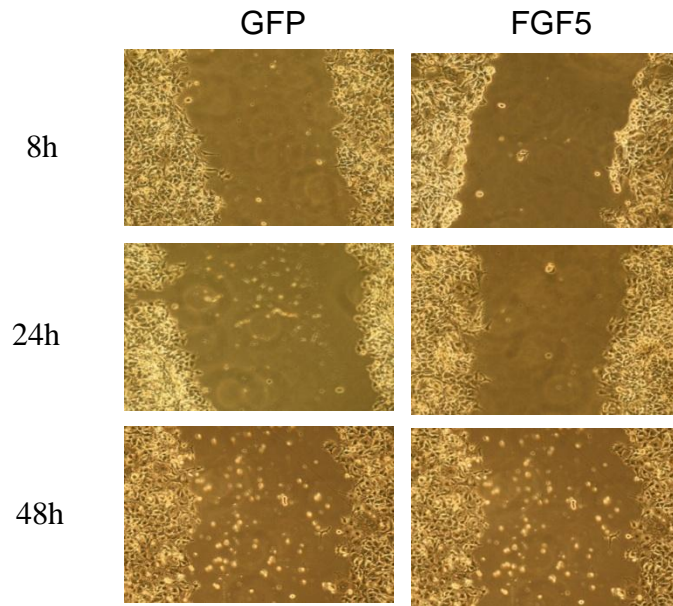


Figure 23: Scratch assay of the VM21 cell line over-expressing FGF5 after 8, 24 and 48 h. Cells did not migrate properly.

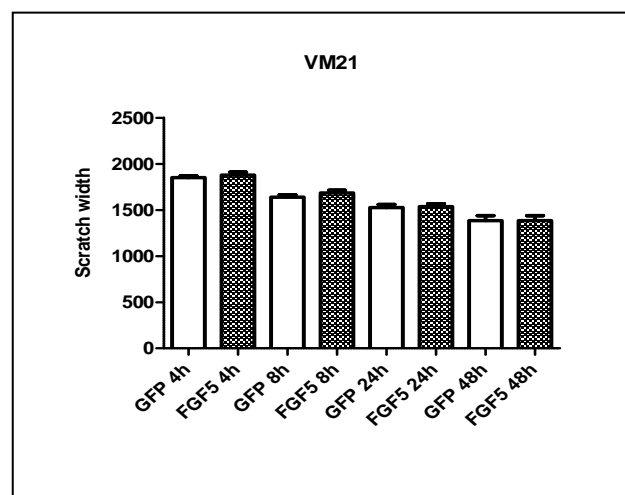


Figure 24: Result of migration of VM21 cells expressing FGF5 after 4, 8, 24, 48 h. VM21-GFP cells were taken as a control.

Results clearly show that FGF5 over-expression in VM1 cells has an impact on migration of cells. On the other hand in VM21 cells FGF5 up- regulation showed less stimulatory effects on migration.

4.3.6 Invasion assay

As described in the methods section, invasive cells are able to break down collagen and thus migrate through the pores of the membrane to the lower chamber. For this experiment just the cells with higher migration ability (VM1) were taken into consideration (Figure 25). The VM21 cell line was not further investigated, because cells did not migrate properly.

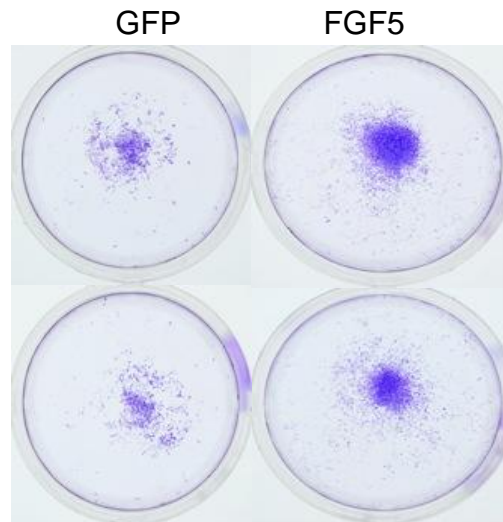


Figure 25: Invasion ability was tested with collagen-coated transwell chambers for the VM1 cell line. Cells were allowed to migrate to the lower chamber for 72 hours. Experiments were done in duplicates. Cells that migrated through the membrane and dropped to the bottom of the well were stained by crystal violet afterwards.

Based on these results, over-expression of FGF5 stimulated cell migration through a collagen matrix (Figure 26).

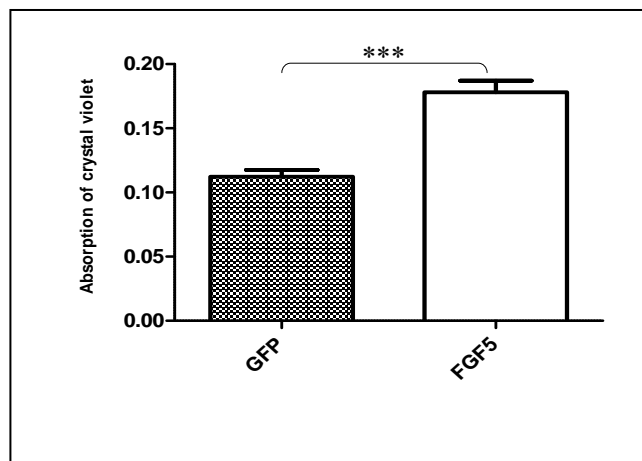


Figure 26 : Photometric measurement of the crystal violet absorption in VM1 cells with FGF5 over-expression that had formed colonies in the lower chamber of the transwell assay. Colony formation was strongly increased for VM1 cells with FGF5 in contrast to GFP control cells. ***p value < 0.001

4.4 HET-CAM assay (*ex vivo*)

To determine the contribution of FGF5 to melanoma cell-induced angiogenesis, the different over-expressing cell models were used in a hen's egg chorioallantoic membrane assay. Recruitment of blood vessels by the growing tumor cells was monitored between embryonic days 7 and 11 and subsequently CAMs were processed for histology to screen for vessel growth and potential tumor cell invasion (Figure 27). The VM21 cell line with over-expressed FGF5 and the respective GFP control cell line were used for this assay. Figure 27 shows an example, where increased recruitment of blood vessels by VM21-FGF5 cells can be observed.

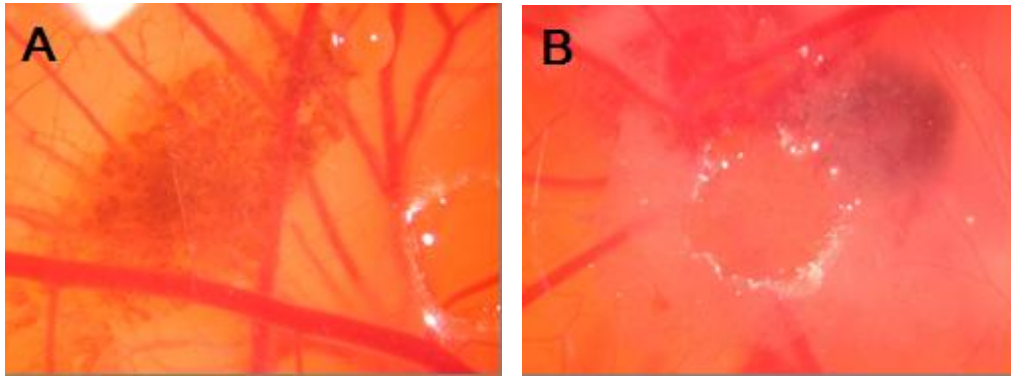


Figure 27: A) Micrograph showing VM21-FGF5 cells on top of a hen's egg CAM on embryonic day 8 as well as blood vessel recruitment by the tumor cells. In contrast, control cells transfected with the GFP construct, (B) recruit fewer blood vessels.

4.4.1 Immunohistochemical staining of hen's egg CAM

HE staining showed that the tumor is placed on top of the hen's egg CAM. Staining of hen's egg CAM with Ki-67 showed proliferation of growing tumor cells on the hen's egg CAM (Figure 28).

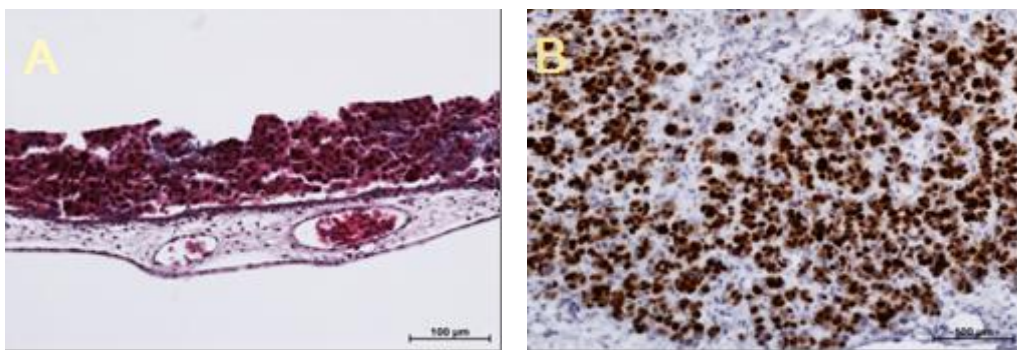


Figure 28: Histological and immunohistochemical demonstration of VM21 tumor cell growth on a hen's egg CAM. A) HE staining, B) Ki-67 cell proliferation staining.

Staining of hen's egg CAM with anti-vWF antibodies showed clearly the endothelial cells (Figure 29).

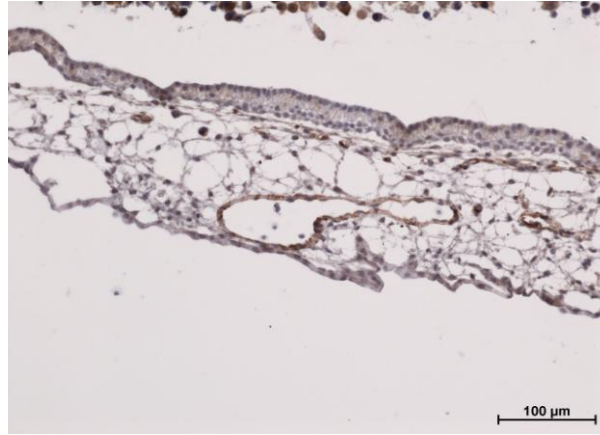


Figure 29: A hen's egg CAM was stained using anti-vWF antibody for demonstration of the FGF5 contribution in recruitment of blood vessels.

4.5 *In vivo* tumor growth

To investigate the impact of FGF5 on tumor growth *in vivo*, VM21-FGF5 and VM21 control cells were injected subcutaneously into severe combined immunodeficient (SCID) mice and tumor growth was recorded. Compared to the mock transfected controls VM21-FGF5 cells formed palpable tumors earlier and tumor volume was increased (Figure 30).

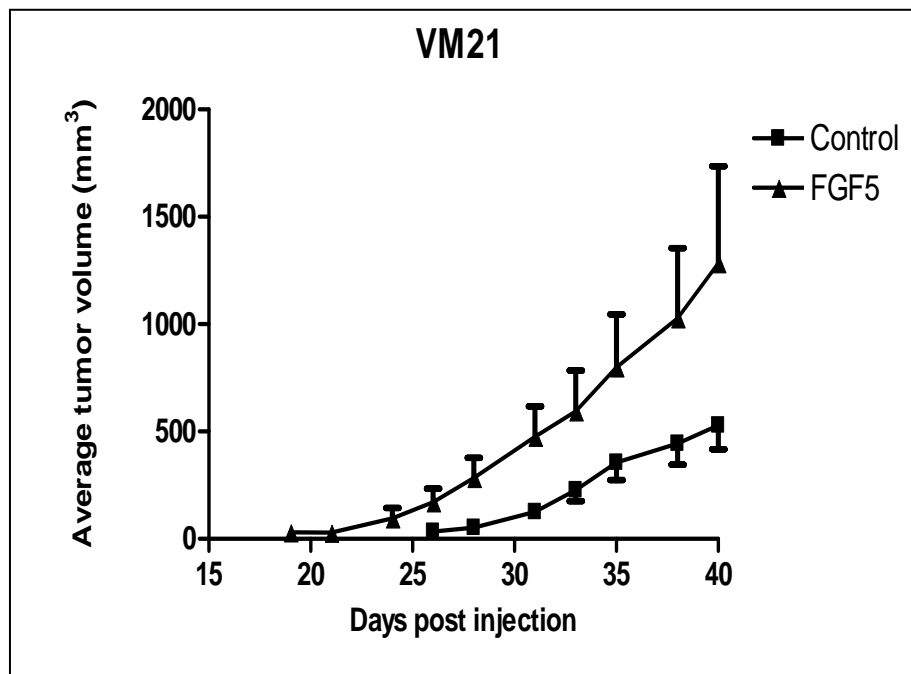


Figure 30 : VM21-FGF5 or VM21-Control cells were subcutaneously injected into the flanks of SCID mice (10^6 cells per mouse, 4 mice per group) and tumor growth was recorded over 40 days. Tumor volume was calculated as $\text{smaller diameter}^2 \times \text{larger diameter} \times 0.5$.

According to the results shown in figure 19, tumor volume in VM21- FGF5 Cells was increased in contrast to mock transfected controls. This was also obvious, when the tumors were dissected out after sacrificing the mice (Figure 31).

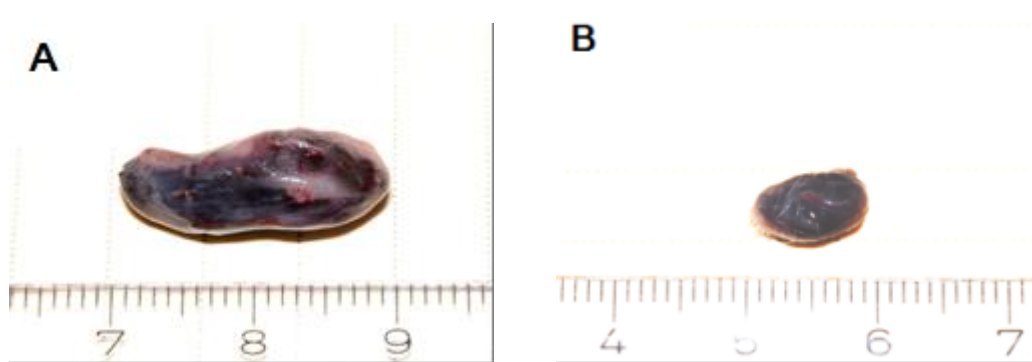


Figure 31: Examples of the impact of FGF5 on tumour growth. A) Xenograft tumor from a mouse with VM21-FGF5, B) tumor from a control mouse engrafted with VM21-GFP cells.

4.5.1 Immunohistochemical staining of VM21 xenograft tumors

HE Staining

This staining gives an overview of the structure of the tissue. Tumor cell necrosis was observed in the central part of the tumor (Figure 32).

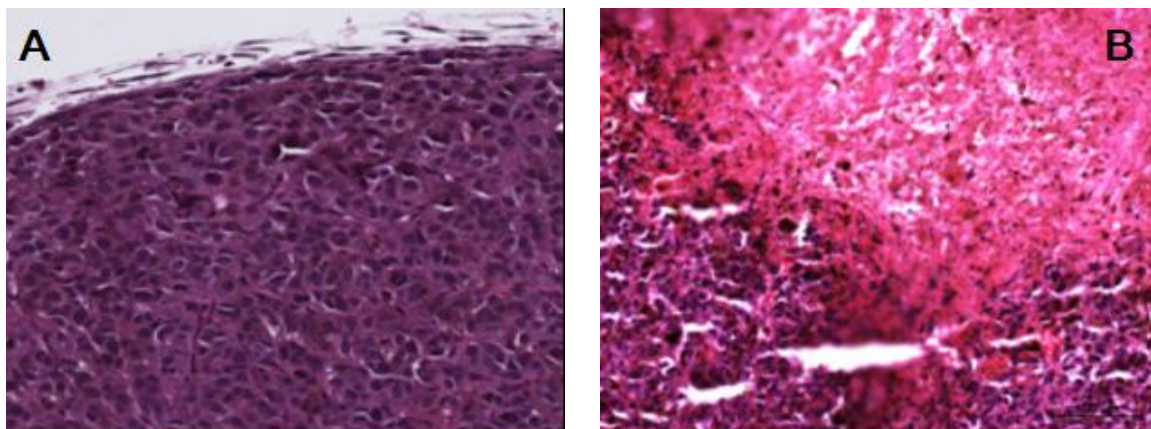


Figure 32 : Examples of histological sections of tumors xenografted VM21 cells A) the nuclei stain blue, dark violet to black. Cytoplasm, collagen, keratin and erythrocytes stain red. B) Histological specimen of tumor stained with HE shows necrosis in some parts of the tumor.

Ki-67 staining

The Ki-67 protein is a cellular marker for proliferation. It is strictly associated with cell proliferation during late G1, S, G2 and M stages of cell cycle. Ki-67 staining of the xenografted tumors demonstrated a high rate of cell proliferation especially at the tumor margins (Figure 33).

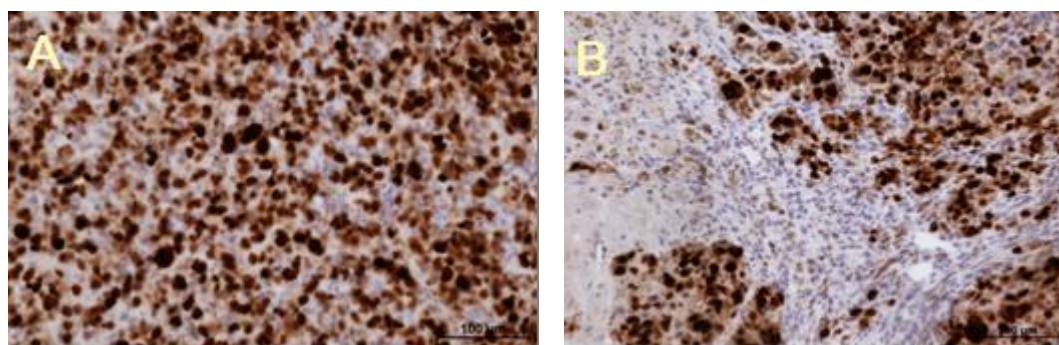


Figure 33 : A and B, Ki-67 cell proliferation staining of a tumor from VM21-FGF5 cells.

von Willebrand Factor (vWF) Antibody Staining

Endothelial cells were identified by staining for von Willebrand factor (vWF) (Figure 34).

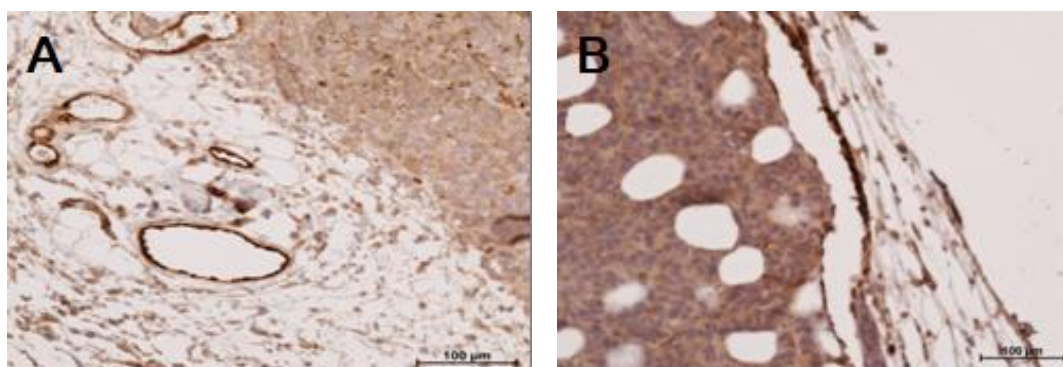


Figure 34: A and B von Willebrand factor (vWF) staining in a mouse engrafted with VM21-FGF5 cells

4.6 HE staining of organs from mice engrafted with VM21-FGF5 or VM21-GFP

Organs (lung, liver) from the xenotransplanted mice were formalin-fixed and stained with HE and Ki-67 in order to detect potential metastases derived from the xenografted tumors. However, staining of lung and liver indicated no metastatic cells in these organs (Figure 35).

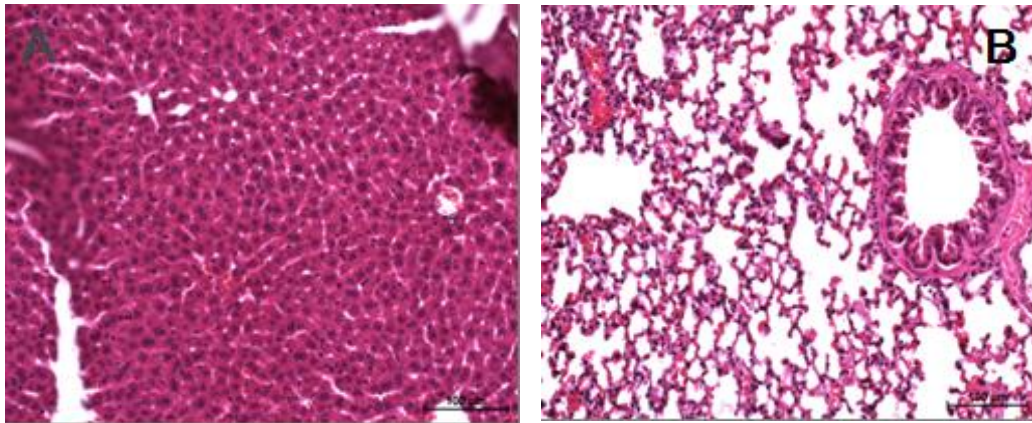


Figure 35 : HE staining of A) Liver B) Lung of mice bearing VM21-FGF5 tumors. Nuclei are stained blue, the cytoplasm and extracellular matrix have varying degrees of pink staining.

4.7 Lentiviral shRNA-mediated knockdown of endogenous FGF5

To investigate the effects of down regulated FGF5 expression, melanoma cells with high endogenous FGF5 expression (VM8, VM7 and VM47) were transduced with shRNA against FGF5. Five different hairpins were tested and a scrambled hairpin with no known cellular target was used as control. Puromycin resistance was used as selection marker. The knockdown of the endogenous FGF5 mRNA level was analyzed via qRT-PCR, using beta 2 microglobulin as house-keeping gene (Figure 36).

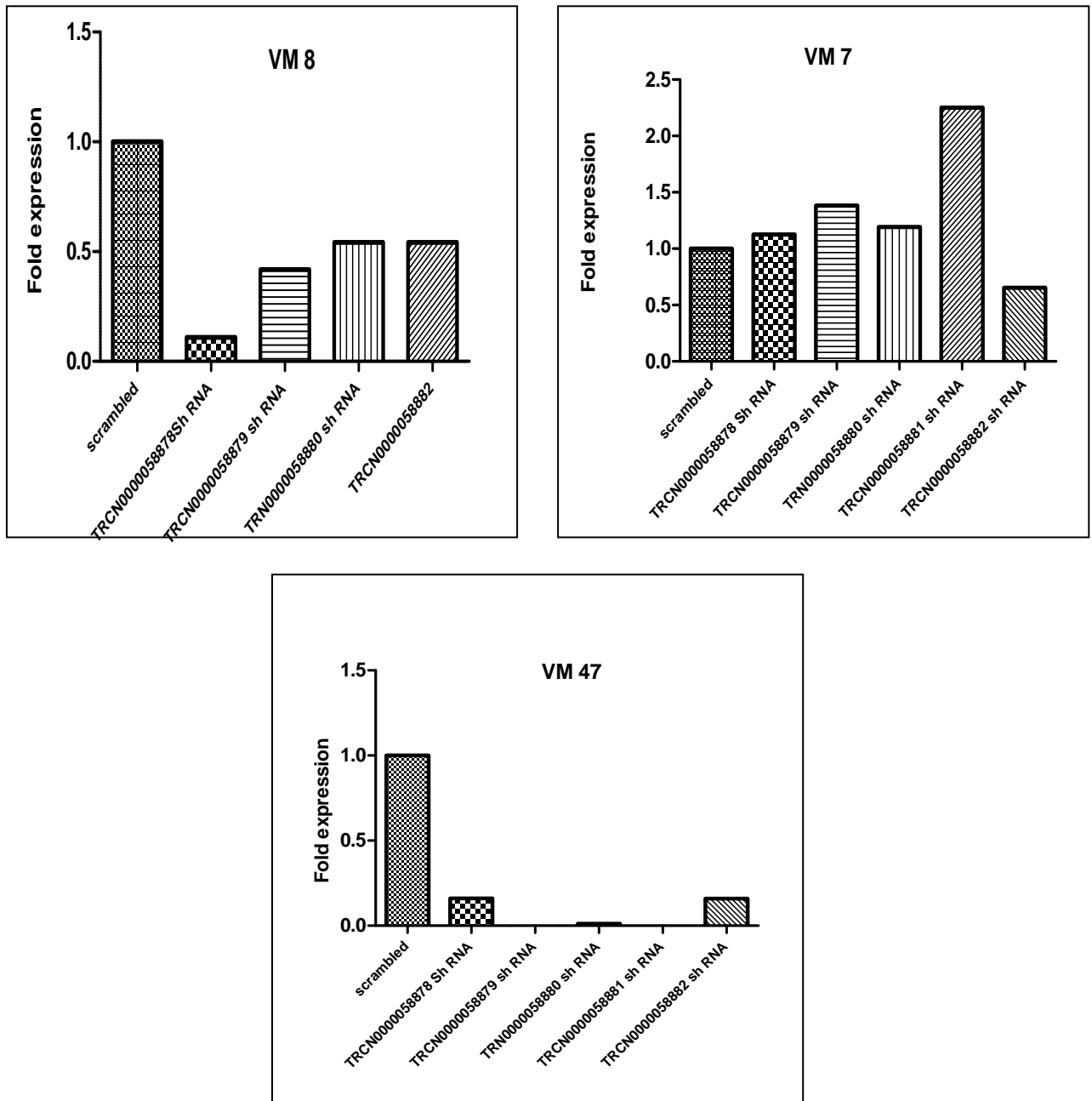


Figure 36: The knockdown of the endogenous FGF5 mRNA level was analyzed by qRT-PCR in melanoma cell lines (VM7, VM8, and VM47).

Based on the data from the real-time PCR, the VM8 cell line transfected with the (TRCN0000058879 sh RNA) hairpin was chosen for further analysis. In VM7 (GTBS) cells no sufficient silencing of FGF5 could be achieved and VM47 (HOST) cells did not grow robustly enough under puromycin selection to allow further experiments.

4.8 Impact of down-modulation of endogenous FGF5 *in vitro*

4.8.1 Effect of shRNA-mediated FGF5 down modulation on proliferation and viability of cells.

To analyze the effect of FGF5 on cell proliferation and viability, VM8 cells were seeded and proliferation of cells was determined in a growth curve experiment.

In comparison to the scrambled control, knockdown of endogenous FGF5 affected cell proliferation and reduced proliferation of cells after five days (Figure 37).

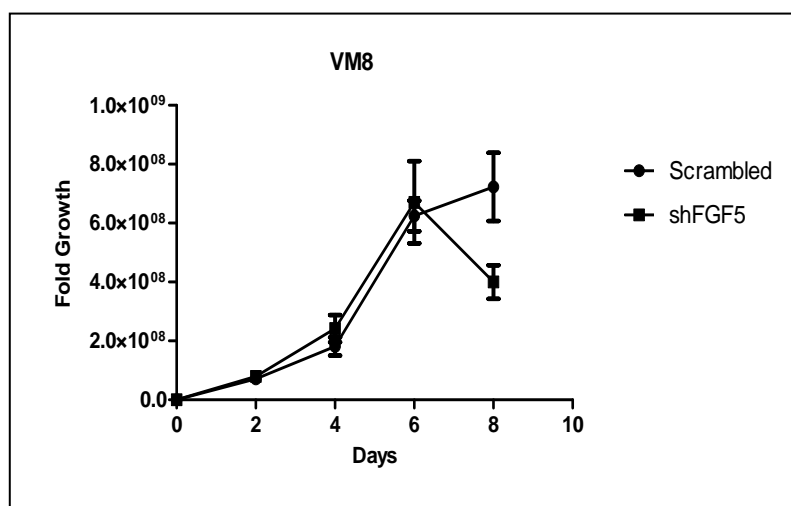


Figure 37: Proliferation of the VM8 cell line with FGF5 down-regulation determined by the Casy cell counter. Cells transfected with a scrambled shRNA were taken as control.

To determine whether FGF5 knock-down has any effect on cell viability, VM8 cells were seeded in RPMI medium with 0.1% FBS and 10% FBS and cell viability was assessed by MTT assay after 5 days. Viability analyses by MTT showed no significant impact of FGF5 silencing on viability of cells in comparison to cells transfected with scrambled shRNA (Figure 38).

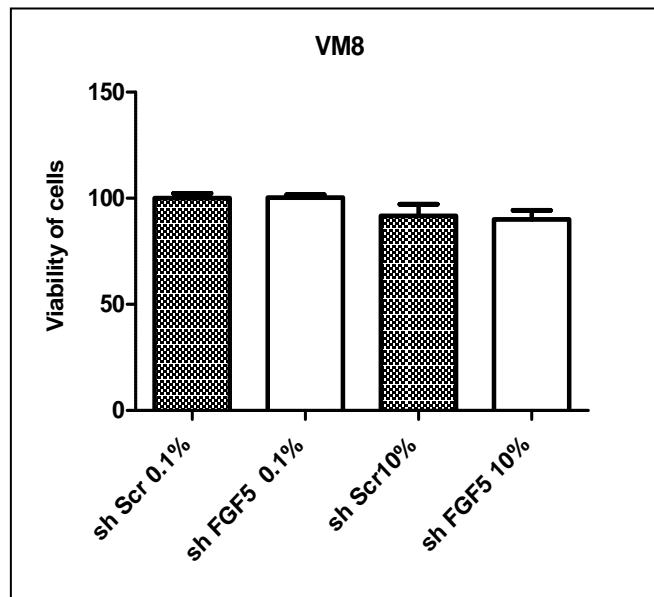


Figure 38: viability of VM8 cell line with FGF5 down regulation incubated in RPMI medium with 0.1 and 10% FBS concentration for 5 days.

4.8.2 Effect of siRNA-mediated FGF5 down-modulation on clonogenicity

5000 VM8 cells were plated in 6-well plates for clonogenicity assays. After approx. 8 days, colonies formed were fixed and stained. The colony formation was reduced for VM8 cells transduced with shFGF5 in comparison to the scrambled shRNA control (Figure 39).

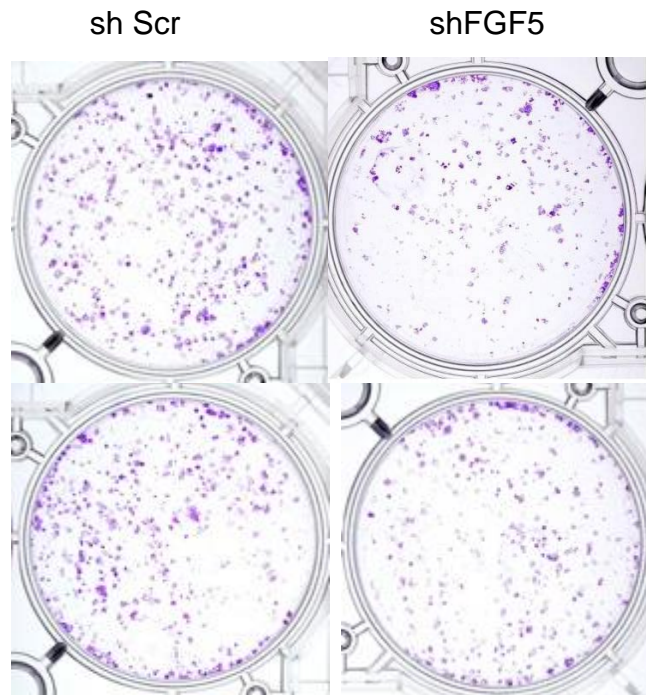


Figure 39 : Effect of shRNA-mediated knockdown of endogenous FGF5 on colony formation. VM8 cells were seeded at low densities (5000 cells/well). Colony formation was determined after about 8 days. Two independent experiments were performed.

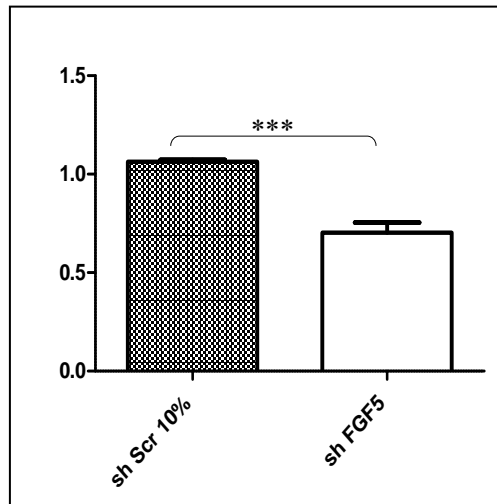


Figure 40: Results of crystal violet absorption showed a reduction in clonogenicity in VM 8 cells transfected with FGF5 shRNA compared to scrambled shRNA- transfected cells. ***p < 0.001.

4.8.3 Effect of shRNA-mediated FGF5 down-modulation on invasion of cells

To test the effect of FGF5 down-modulation on invasion and migration of cells, 40000 VM8 cells with silenced FGF5 were seeded and incubate for 72 h. Only those cells able to migrate through the collagen coated membrane and settle on the bottom of the well were incubated for further 3 days. The colonies of these cells were fixed and stained by crystal violet afterwards (Figure 41). The results showed that colonies of FGF5 down regulated VM8 cells are fewer but have a larger size in contrast to control cells. Based on measurement of crystal violet absorption, more FGF5 knock down cells than control cells are present in the wells at the end of the experiment (Figure 42).

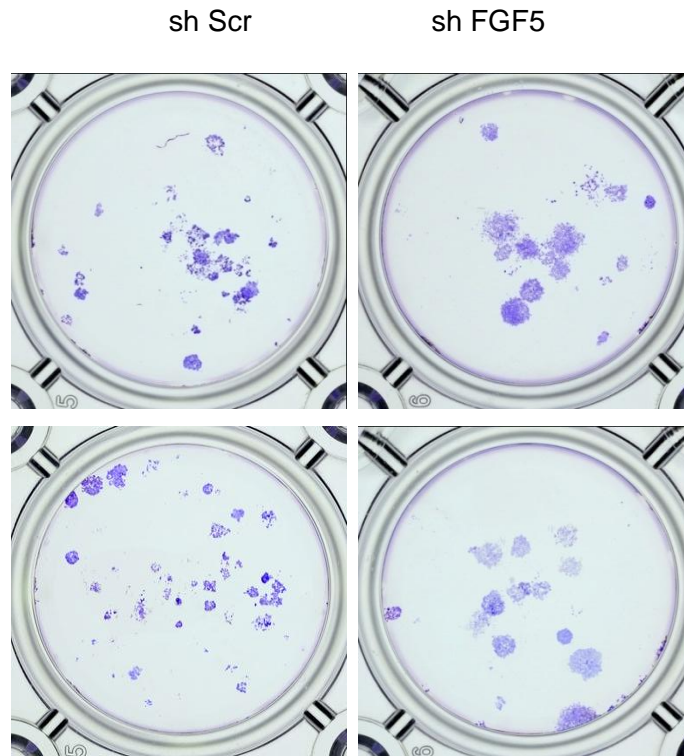


Figure 41: Invasion ability of VM8 cells with down-regulated FGF5 was tested. 40000 cells/well were seeded into collagen matrix-coated transwell chambers and incubated for 72 hours. Cells in the lower chamber were stained by crystal violet afterwards. At least two independent experiments in duplicates were performed.

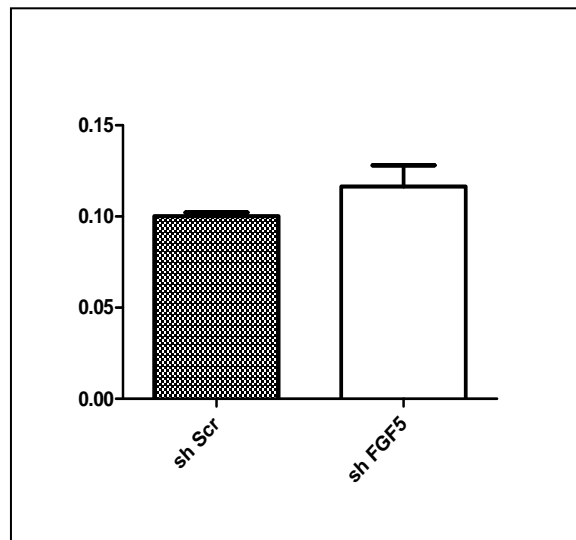


Figure 42: Results of photometric measurement of the crystal violet absorption of VM8 cells with silenced FGF5 and control cells after migration through a collagen matrix.

4.9 Treatment of melanoma cells with *Neurolena lobata* extract

The aim of this part of the study was to test the inhibition effect of a plant extract from *N. lobata* on melanoma cell lines. *N. lobata* belongs to the family *Asteraceae*. *Asteraceae* is the largest family of flowering plants and spread worldwide. It is divided into 11 subfamilies of which the subfamily *Asteroideae* comprises approximately 70 % of specific diversity of the whole family. Since 2004, this subfamily is divided into three supertribes [91] of which *Helianthodae* comprises the species *N.lobata*. This plant is spread in Latin American countries and can be found especially in Guatemala and Costa Rica. It has been suggested that *N. lobata* extract has an inhibition effect on the expression of receptor tyrosine kinases at the transcription level. For this purpose five melanoma cell lines (VM1, VM21, VM24 and VM48) were seeded in 96-well plates and incubated overnight. Next day the cells were treated with different concentration of *N. lobata* extract and incubated for 5 days. After that viability of the cells was measured by MTT assay (Figure 43).

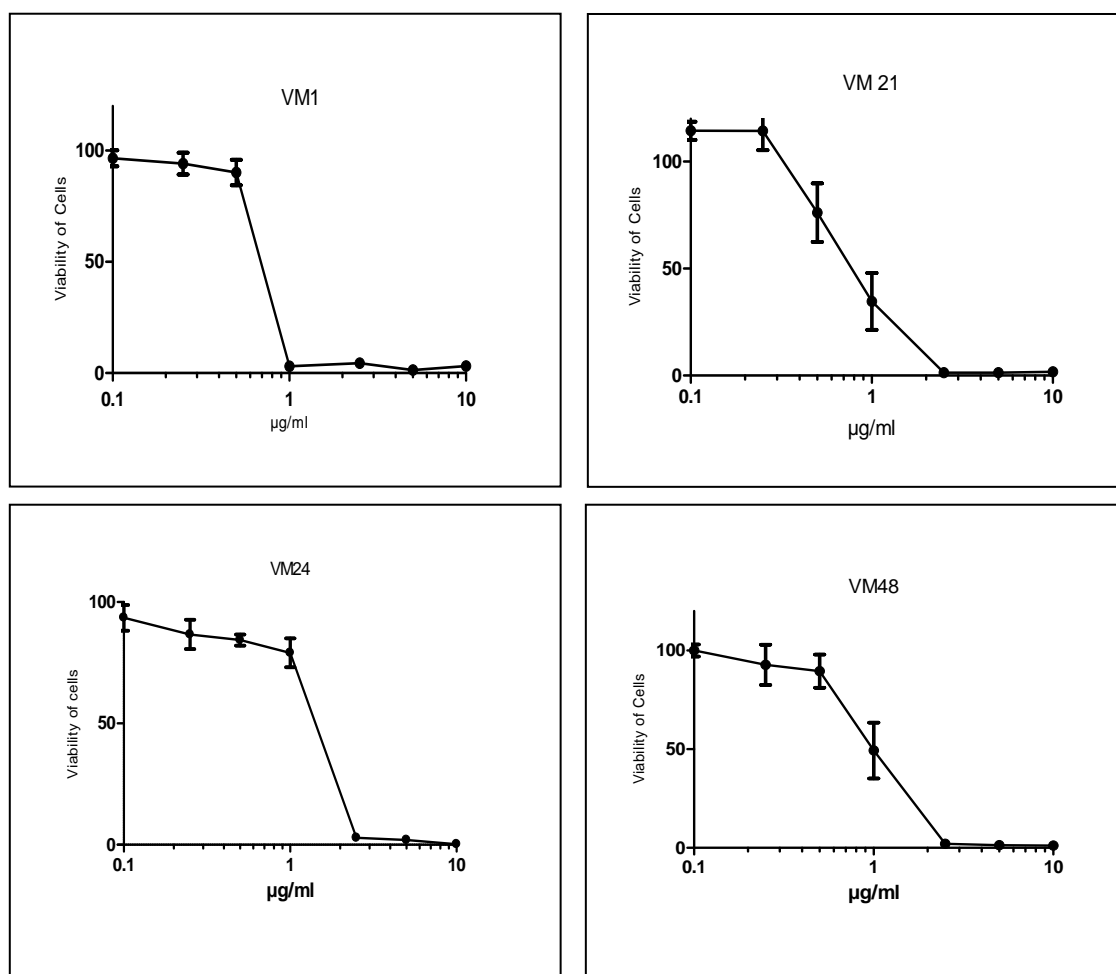


Figure 43 : MTT assay of the four melanoma cell lines VM1, VM21, VM24 and VM48. 3000cells per well were treated with *N. lobata* extract and incubated for 5 days.

Results showed that *N.lobata* extract has a concentration-dependent toxic effect in all four tested melanoma cell lines.

4.9.1 Effect of *N. lobata* on FGF/FGFR expression

Since *N. lobata* extract was suggested to influence the transcription of specific genes, it was tested, whether treatment with *N.lobata* extract has an impact on the expression of FGFR1, FGFR4 or FGF2 in melanoma cells. VM21 cells were treated with 5 μ g/ml *N. lobata* extract for 24 h. qRT-PCR of FGFR1, FGFR4 and FGF2 was performed in these cells (Figure 44).

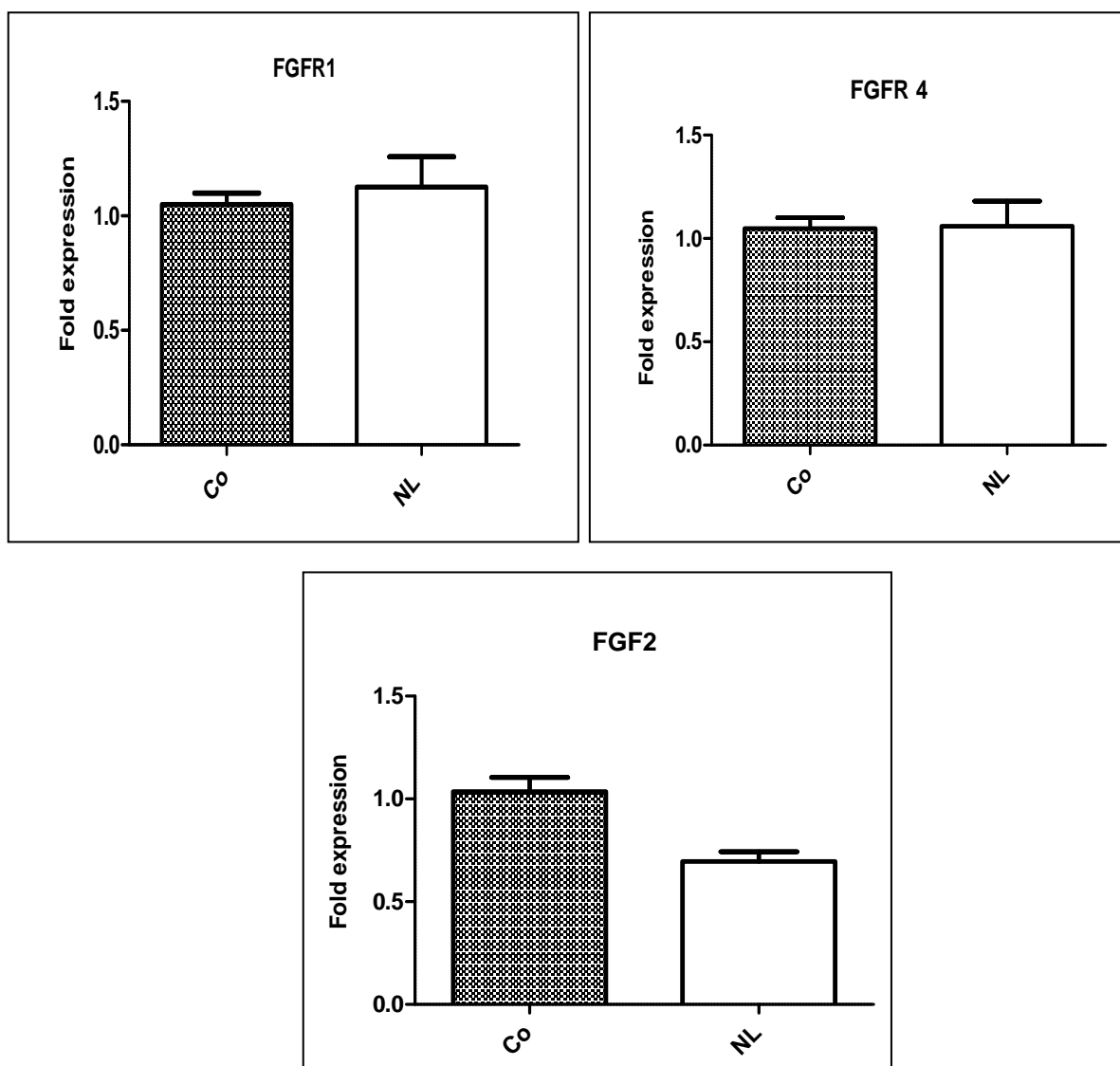


Figure 44: Quantitative expression analysis (qRT-PCR) of FGFR1, 4 and FGF2 in the VM21 cell line after treatment with 5 μ g/ml *N. lobata* extract (NL). The DMSO control (Co) was taken as reference. Beta-2 microglobulin was used as house-keeping gene.

Expression analysis by qRT-PCR revealed no significant difference in expression of FGFR1 and 4 in cells after treatment with *N. lobata* extract compared to DMSO treated control cells, whereas a reduction of FGF2 expression was observed in cells with *N. lobata* treatment in contrast to DMSO-treated cells.

5 Discussion

The fibroblast growth factor (FGF) signaling system is involved in normal cell growth survival, differentiation, and angiogenesis. Thus, deregulated FGF/FGFR-mediated signalling has been implicated in carcinogenesis. Over-expression of growth and survival promoting factors is an important hallmark of neoplastic cells and a major driving force for tumor progression and dissemination. Over-expression of FGF ligands has been identified in a great variety of human tumors.

There are some possibilities how to release FGF: first, FGFs may be overexpressed and secreted by the tumor cells themselves; for example FGF2 mRNA has been shown to be expressed in over 94% of human gliomas [83] however, the FGF-2 protein has not been detected in normal brain by immunohistochemistry [80]. The expression of FGF-2 has also been shown positively to correlate with the degree of malignancy and vascularity in human gliomas [80].

Secondly, FGFs may be secreted by the stromal cells in response to a signal from the tumor cells; an example for this possibility is illustrated with FGF5 in pancreatic cancer. FGF3, 4 and 8 which are normally not expressed to high levels in adult tissues have been found in a number of human neoplasms, for instance in Kaposi's sarcoma, and in carcinomas of the breast, prostate, ovary and esophagus [81-84].

Expression of FGF2 has been identified as important characteristic of melanoma cells in contrast to normal melanocytes [85] and has been linked to tumor progression in melanoma and multiple other malignancies [86].

An autocrine growth stimulatory role for FGF2 in melanoma has been clearly shown through inhibition of FGF2 activity by intracellular injection of blocking antibodies [84, 74]. Expression analysis showed that FGFR1 and FGFR4 are highly expressed in nearly all melanoma cell lines, compared to FGFR2 and FGFR3. Recent studies in melanoma revealed that tumor growth or cell proliferation is reduced to about 50%, when infected with adenoviruses bearing dnFGFR1 constructs, compared to GFP as control [75]. In a previous study, very low expression of FGF5 in melanocytes and 90% over-expression of FGF5 in the majority of the tested melanoma cell lines was found [28].

5.1 Impact of FGF5 on the malignant phenotype *in vitro*

In the present study, two melanoma cell lines (VM1, VM21) with low endogenous FGF5 expression were stably transfected with a vector containing human FGF5, GFP and an IRES-binding site from a bicistronic mRNA as well as a G418 resistance marker and the impact of FGF5 over-expression on the malignant phenotype of melanoma was characterized in these cell lines by subjecting them to different *in vitro* assays.

Results of the scratch assay clearly showed the influence of FGF5 over-expression to result in a more migratory phenotype in the VM1 cell line, in agreement with a recent study, demonstrating that FGF5 stimulates migration of glioblastoma cell lines [44]. On the other hand in VM21 cells FGF5 up-regulation showed less stimulatory effects on migration in the scratch assay. In invasion assays only the cells with higher migration ability (VM1) were taken into consideration and the impact of FGF5 on migration ability of cells through a collagen matrix was demonstrated.

An increased clonogenicity was observed in VM1 cells with FGF5 over-expression compared to GFP control. Again, in the VM21 cell line colony formation was not significantly influenced by FGF5. No significant impact on the ability of cells expressing FGF5 to form clones was observed in soft agar in contrast to cells with the GFP construct. The MTT assay showed a decrease in viability of cells with FGF5 over-expression in RPMI medium with 0.1% FBS. A slight increase in viability of VM1 in medium with 10% FBS was observed, whereas in VM21 cells no difference was detected. The decreased viability of cells with FGF5 over-expression in medium with low serum was unexpected and the reason is not clear.

Relating to effects of FGF5 over-expression on proliferation of VM1 and VM21 cells, no difference was observed in contrast to GFP over-expressing cells. Thus, FGF5 over-expression did not stimulate melanoma cell proliferation *in vitro*.

5.2 Hen's egg chorioallantoic membrane (HET-CAM)

The purpose of this assay was to determine the contribution of FGF5 to melanoma cell-induced angiogenesis. Results show the recruitment of blood vessels by the growing tumor cells (VM21 cells with FGF5 over-expression) on top of a hen's egg CAM. FGF5 may exert paracrine effects on vascular endothelial cells that are mediated through FGFRs 1 and 2, the main FGFRs on endothelial cells [28].

FGF5 was recently recognized as a potent inducer of tube formation of endothelial cells [43]. It was also demonstrated that tumor cell-derived FGF5 induces differentiation in human umbilical cord endothelial cells *in vitro* with an activity similar to vascular endothelial growth factor (VEGF) and stimulates the growth of vascular endothelial cells [49]. VEGF and basic fibroblast growth factor (bFGF, FGF2) are recognized as stimulators of migration and angiogenesis during the progression of melanoma [88]. The present study may confirm the role of FGF5 as an important player in melanoma cell-induced angiogenesis. The quantification of the HET-CAM data, however, is challenging and the method still needs to be improved to allow a statistical comparison between FGF5 over-expressing and GFP over-expressing melanoma cells.

5.3 Lentiviral shRNA-mediated knockdown of endogenous FGF5

In our study, silencing of FGF5 with lentiviral siRNA in VM8 cells, which have a high level of endogenous FGF5, reduced cell proliferation after five days in contrast to cells with control shRNA. While, as mentioned above, FGF5 over-expression did not induce an increase in cell proliferation *in vitro*. Results are in agreement with data from the literature showing that siRNA-mediated FGF5 down-modulation reduced glioblastoma cell proliferation [43]. Viability analyses by MTT assay, however, showed no significant impact of FGF5 silencing on viability of cells in comparison to cells transfected with scrambled shRNA. In clonogenicity assays, the formation of colonies was reduced for VM8 cells when FGF5 was silenced by shRNA. It is presumed that the down modulation of FGF5 reduced clone formation in the clonogenic assay. Relating to migration ability of cells with shRNA-mediated FGF5 silencing, measurement of crystal violet absorption shows no significant effect of FGF5 down-regulation on invasion ability of cells in contrast to cells expressing scrambled shRNA.

Taking these results together, shRNA-mediated knockdown of endogenous FGF5 appears to have an inhibitory effect on cell proliferation and colony formation *in vitro*.

5.4 *In vivo* tumor growth

The impact of FGF5 on tumor growth *in vivo* was tested by a xenotransplantation experiment in SCID mice. VM21 melanoma cells with FGF5 over-expression and respective control cells were injected subcutaneously into the flanks of SCID mice. The results clearly show that VM21-FGF5 formed palpable tumors earlier and tumor

volume was increased in contrast to mock transfected controls. This result supports the hypothesis that FGF5 over-expression contributes to the malignant phenotype of melanoma cells and results in more aggressive tumor growth. This is the first study to demonstrate increased tumor growth as a result of FGF5 over-expression *in vivo*. In other studies it has been shown that FGF8b-transfected MCF-7 human breast cancer cells formed faster growing tumors than vector-only-transfected cells when xenografted into nude mice [86].

HE staining of tumors showed tumor cell necrosis in the central part of the tumor. Results of Ki-67 staining demonstrated a high rate of cell proliferation especially at the tumor margins. Endothelial cells were identified by staining for von Willebrand factor (VWF) in tumors. Identification of endothelial cells in tumors correlated with the finding that tumor angiogenesis activates endothelial cell proliferation, recruits migrating endothelial cells and pericytes, and forms new blood vessels through vascular remodeling and maturation [89]. In HE and Ki-67 stainings of lungs and livers of xenotransplanted mice no incidence of potential metastases derived from the xenografted tumors was observed.

5.5 Treatment of melanoma cells with *Neurolena lobata* extract

Results of MTT assay showed that *N. lobata* extract has a concentration-dependent cytotoxic effect in all four tested melanoma cell lines. Although only few studies are available on cytotoxicity of *N. lobata*, our data are consistent with the studies, which revealed that lobatin B of *N. lobata* was the compound with the strongest cytotoxic activity in GLC4 and COLO 320 tumor cell lines [90]. Recently *N. lobata* extract was shown to inhibit expression of the NPM/ALK fusion oncogene present in a high fraction of anaplastic large cell lymphomas (ALCL) [91]. Whether the observed reduction of FGF2 expression in VM21 cells contributes to the cytotoxicity of *N. lobata* extract in melanoma cells remains to be determined. Expression analysis showed no significant difference in expression of FGFR1 and 4 after treatment with *N. Lobata*.

6 Appendix

6.1 List of Figures

Figure 1: Location of melanocytes and keratinocytes in human skin [4].	12
Figure 2: Factors suggested to influence melanoma development [8].	13
Figure 3: Dynamics of intercellular interactions under normal and pathological situations during melanoma development. (a) Normal melanocytes reside close to the basement membrane and form an 'epidermal melanin unit' that contains one melanocyte and five to eight keratinocytes. Melanocytes interact with adjacent keratinocytes through E-cadherin, desmoglein 1, and connexins. This contact-dependent interaction is required for the growth and phenotypic control of melanocytes by keratinocytes. (b) Malignant melanoma cells proliferate, penetrate basement membrane, and invade into dermis. A shift of cadherin profile from E to N during melanoma development not only frees the cells from epidermal keratinocytes, but also confers new adhesive properties. Melanoma cells form N-cadherin-mediated adhesion and connexin-mediated gap junctions with N-cadherin-expressing fibroblasts, endothelial cells, and adjacent melanoma cells. Mel-CAM and its unknown ligand are also involved in melanoma-melanoma cell interaction, which is implicated to play a role in the progression of melanoma [11].	14
Figure 4: Melanoma signaling networks. Shown is a simplified diagram of three of the major genetic networks involved in melanoma tumorigenesis, survival, and senescence. Included in the NRAS signaling network (green) are the MAPK and the PI3 Kinase/AKT pathways, which have been implicated in melanoma proliferation, survival, and progression. The CDKN2A locus encodes two separate tumor suppressors, p16 and p14ARF, both of which are thought to contribute to senescence and tumor growth restriction. The p53/Bcl-2 signaling network (red) is a major contributor to melanoma apoptosis and chemosensitivity and is regulated by many of the oncogenic melanoma pathways. At the top of the figure selected therapeutic agents that target each of these genetic networks are shown [25].	16
Figure 5: Members of the human fibroblast growth factor (FGF) gene family [34].	18
Figure 6: Structure of FGF receptors [56].	21
Figure 7: Overview of variants of FGF-seceptors generated by the mechanism of alternative splicing. Concerning the FGFR-2 gene, Ig domain IIIb is pre-dominantly expressed in the epithelial lineage, while Ig IIIc domains are only expressed in the mesenchymal lineage [55, 56, 57].	21
Figure 8: Protein structure of FGFRs. FGFRs is receptor tyrosine kinases consisting of cytoplasmic interrupted kinase domains and transmembrane domains with high degrees of homology between different FGFRs. The extracellular domains consist of three immunoglobulin (Ig)-like loops that bind FGFs between Ig-loop 2 and 3. FGFRs 1-3 are subject to alternative splicing events that affect Ig-loop 3 and therefore have large effects on the receptors ligand specificity. HSPGs mediate receptor-ligand binding [28].	22
Figure 9: Overview of oncogenic signal cascades activated by FGFs [59].	23
Figure 10: Example of calibration curve used for determination of protein concentration by	30
Figure 11: PIRESEGFSEGFPlig vector containing the FGF5 cDNA.	33
Figure 12: Quantitative expression analysis (qRT-PCR) of FGF5 in a panel of human melanoma cell lines (VM) compared to primary human melanocytes (PM). Strong over-expression (10-9000 fold) of FGF5 was seen in 9 of 17 melanoma cell lines [73].	39
Figure 13: Quantitative expression analysis of FGF5 mRNA in VM1 and VM 21 cell lines, taking the	40
Figure 14: FGF5 protein expression was examined by western blot in the FGF5-transfected VM1 and VM21 cell line and GFP control cells. Specific FGF5 bands were detected at 30 kDa whereas β -actin bands were detected at 42 kDa.	40
Figure 15: Viability of melanoma cell lines VM1 and VM21 with FGF5 over-expression incubated in RPMI medium with 0.1 or 10% FBS for 5 days. The GFP control was taken as reference. * $p < 0.05$, ** $p < 0.01$.	41
Figure 16: Proliferation of melanoma cell lines (VM1, VM21 expressing FGF5 determined by the Casy	41
Figure 17: Examples of clonogenic assays of transfected VM1 and VM21 cell lines. Cells were	42
Figure 18: Photometric measurement of the crystal violet absorption in VM1 and VM21 cell lines showing a difference in clonogenicity of VM1 with over-expressed FGF5 compared to GFP.* $p < 0.05$ No difference was observed in colony formation of VM21 cells.	43
Figure 19: VM1 and VM21 cells with over-expressed FGF5 were plated in soft agar at a density of 10000 per 6-well. Clones formed under anchorage-independent conditions were evaluated after approx. 4 weeks of incubation.	43
Figure 20: Results of soft agar assays. VM1 and VM21cell lines were tested.10 000 cells were seeded. Four different areas per well were counted.	44
Figure 21: Example of a scratch assay of the VM1 cell line with over-expressed FGF5, after 8, 24 and 48h	45

Figure 22: Results of relative Migration of VM1 cells expressing FGF5 after 4, 8, 24, 48h. GFP cells were taken as a control.	45
Figure 23: Scratch assay of the VM21 cell line over-expressing FGF5 after 8, 24 and 48 h. Cells did not migrate properly.	46
Figure 24: Result of migration of VM21 cells expressing FGF5 after 4, 8, 24, 48 h. VM21-GFP cells were	46
Figure 25: Invasion ability was tested with collagen-coated transwell chambers for the VM1 cell line. Cells were allowed to migrate to the lower chamber for 72 hours. Experiments were done in duplicates. Cells that migrated through the membrane and dropped to the bottom of the well were stained by crystal violet afterwards.	47
Figure 26: Photometric measurement of the crystal violet absorption in VM1 cells with FGF5 over-expression that had formed colonies in the lower chamber of the transwell assay. Colony formation was strongly increased for VM1 cells with FGF5 in contrast to GFP control cells. ***p value < 0.001	47
Figure 27: A) Micrograph showing VM21-FGF5 cells on top of a hen's egg CAM on embryonic.....	48
Figure 28: Histological and immunohistochemical demonstration of VM21 tumor cell growth on.....	48
Figure 29: A hen's egg CAM was stained using anti-vWF antibody for demonstration of the FGF5 contribution in recruitment of blood vessels.....	49
Figure 30: VM21-FGF5 or VM21-Control cells were subcutaneously injected into the flanks of SCID	49
Figure 31: Examples of the impact of FGF5 on tumour growth. A) Xenograft tumor from a mouse	50
Figure 32: Examples of histological sections of tumors xenografted VM21 cells A) the nuclei stain blue, dark violet to black. Cytoplasm, collagen, keratin and erythrocytes stain red. B) Histological specimen of tumor stained with HE shows necrosis in some parts of the tumor.	50
Figure 33: A and B, Ki-67 cell proliferation staining of a tumor from VM21-FGF5 cells.	51
Figure 34: A and B von Willebrand factor (vWF) staining in a mouse engrafted with VM21- FGF5 cells	51
Figure 35: HE staining of A) Liver B) Lung of mice bearing VM21-FGF5 tumors. Nuclei are stained.....	52
Figure 36: The knockdown of the endogenous FGF5 mRNA level was analyzed by qRT-PCR in melanoma cell lines (VM7, VM8, and VM47).....	53
Figure 37: Proliferation of the VM8 cell line with FGF5 down-regulation determined by the Casy cell counter. Cells transfected with a scrambled shRNA were taken as control.....	54
Figure 38: viability of VM8 cell line with FGF5 down regulation incubated in RPMI medium with 0.1 and 10% FBS concentration for 5 days.	55
Figure 39: Effect of shRNA-mediated knockdown of endogenous FGF5 on colony formation. VM8 cells were seeded at low densities (5000 cells/well). Colony formation was determined after about 8 days. Two independent experiments were performed.....	55
Figure 40: Results of crystal violet absorption showed a reduction in clonogenicity in VM 8 cells transfected with FGF5 shRNA compared to scrambled shRNA- transfected cells. ***p < 0.001.	56
Figure 41: Invasion ability of VM8 cells with down-regulated FGF5 was tested. 40000 cells/well were seeded into collagen matrix-coated transwell chambers and incubated for 72 hours. Cells in the lower chamber were stained by crystal violet afterwards. At least two independent experiments in duplicates were performed.....	57
Figure 42: Results of photometric measurement of the crystal violet absorption of VM8 cells with silenced FGF5 and control cells after migration through a collagen matrix.....	57
Figure 43: MTT assay of the four melanoma cell lines VM1, VM21, VM24 and VM48. 3000cells per well.....	58
Figure 44: Quantitative expression analysis (qRT-PCR) of FGFR1, 4 and FGF2 in the VM21 cell line after treatment with 5 µg/ml <i>N. lobata</i> extract (NL). The DMSO control (Co) was taken as reference.....	59

6.2 List of Tables

Table 1: FGF-Receptor genes, their chromosomal localizations, splice variants and ligand	18
Table 2: The physiology of FGFs [55].	20
Table 3: Used cell lines, including VM (Vienna Melanoma) numbers, origin and histology.....	26
Table 4: Pipetting Scheme of BSA standards and protein samples. All concentrations were	30
Table 5: Recipes for PAGE gels	31
Table 6: List of antibodies used for immunodetection. Concentration of BSA as diluent was 3%, but.....	32
Table 7: End-concentration of additives during selection and cultivation	33

6.3 Abbreviations

EtOH – Ethanol

FGF - Fibroblast Growth Factor

FGFR - Fibroblast Growth Factor Receptors

FGF-BP - FGF Binding Protein

FRS2 - Fibroblast Growth Factor Receptor Substrate 2

IRES - Internal Ribosomal Entry Site

MAPK - Mitogen Activated Protein Kinase

ERK - Extracellular Signalregulated Kinase

PAGE - Polyacrylamide Gelelectrophoresis

PBS - Phosphate Buffered Saline

ROS - Reactive Oxygen Species

RPMI - Roswell Park Memorial Institute

RT - Room Temperature

SCID - Severe Combined Immunodeficiency

SDS - Sodium Dodecyl Sulfate

TBS - Tris Buffered Saline

TEMED - N,N,N',N'-Tetramethylethylenediamine

Tris - Trishydroxymethyl Aminomethane

6.4 References

- [1] Ito S, Wakamatsu K. Quantitative analysis of eumelanin and pheomelanin in humans, mice, and other animals: a comparative review. *Pigment Cell Res.* 2003 Oct; 16(5):523-31.
- [2] Haass NK, Smalley KS, Li L, Herlyn M. Adhesion, migration and communication in melanocytes and melanoma. *Pigment Cell Res.* 2005 Jun;18(3):150-9.
- [3] Gertrude-E. Costin* aVJH. Human skin pigmentation: melanocytes modulate skin color in response to stress 2007.
- [4] Jean L. Bolognia M, and Seth J. Orlow, MD,. melanocytes.
- [5] Herrling T, Jung K, Fuchs J. The role of melanin as protector against free radicals in skin and its role as free radical indicator in hair. *Spectrochim Acta A Mol Biomol Spectrosc.* 2008 May;69(5):1429-35.
- [6] Jung K, Seifert M, Herrling T, Fuchs J. UV-generated free radicals (FR) in skin: their prevention by sunscreens and their induction by self-tanning agents. *Spectrochim Acta A Mol Biomol Spectrosc.* 2008 May;69(5):1423-8.
- [7] Satyamoorthy K, Herlyn M. Cellular and molecular biology of human melanoma. *Cancer Biol Ther.* 2002 Jan-Feb;1(1):14-7.
- [8] Danen EH, Sonneveld P, Sonnenberg A, Yamada KM. Dual stimulation of Ras/mitogen-activated protein kinase and RhoA by cell adhesion to fibronectin supports growth factor-stimulated cell cycle progression. *J Cell Biol.* 2000 Dec 25;151(7):1413-22.
- [9] Gruss C, Herlyn M. Role of cadherins and matrixins in melanoma. *Curr Opin Oncol.* 2001 Mar;13(2):117-23.
- [10] Shih Ie M, Hsu MY, Oldt RJ, 3rd, Herlyn M, Gearhart JD, Kurman RJ. The Role of E-cadherin in the Motility and Invasion of Implantation Site Intermediate Trophoblast. Placenta. 2002 Nov;23(10):706-15.
- [11] Li G, Satyamoorthy K, Meier F, Berking C, Bogenrieder T, Herlyn M. Function and regulation of melanoma-stromal fibroblast interactions: when seeds meet soil. *Oncogene.* 2003 May 19;22(20):3162-71.
- [12] Ha L, Merlino G, Sviderskaya EV. Melanomagenesis: overcoming the barrier of melanocyte senescence. *Cell Cycle.* 2008 Jul 1;7(13):1944-8.
- [13] Herlyn M, Ferrone S, Ronai Z, Finerty J, Pelroy R, Mohla S. Melanoma biology and progression. *Cancer Res.* 2001 Jun 1;61(11):4642-3.
- [14] Sharpless WYKaNE. The Regulation of INK4/ARF in Cancer and Aging. review. October 2006
- [15] Campioni M, Santini D, Tonini G, Murace R, Dragonetti E, Spugnini EP, et al. Role of Apaf-1, a key regulator of apoptosis, in melanoma progression and chemoresistance. *Exp Dermatol.* 2005 Nov;14(11):811-8.
- [16] Jordan S Fridman1 aSWL. Control of apoptosis by p53. review. 2003.
- [17] Stuart J Gallagher JFT, James Indsto, Lyndee L Scurr, Margaret Lett, Bo-Fu Gao, Ruth Dunleavy, Graham J Mann, Richard Kefford and Helen Rizos p16INK4a expression and absence of B-RAF are independent predictors of chemosensitivity in melanoma tumors *Journal for Oncology Research.* 2008.
- [18] Willmore-Payne C, Holden JA, Tripp S, Layfield LJ. Human malignant melanoma: detection of BRAF- and c-kit-activating mutations by high-resolution amplicon melting analysis. *Hum Pathol.* 2005 May;36(5):486-93.
- [19] Ball NJ, Yohn JJ, Morelli JG, Norris DA, Golitz LE, Hoeffler JP. Ras mutations in human melanoma: a marker of malignant progression. *J Invest Dermatol.* 1994 Mar;102(3):285-90.

- [20] John A. Curtin PD, Jane Fridlyand, Ph.D., Toshiro Kageshita, M.D., Hetal N. Patel, M.S., Klaus J. Busam, M.D., Heinz Kutzner, M.D., Kwang-Hyun Cho, M.D., Setsuya Aiba, M.D., Ph.D., Eva-Bettina Bröcker, M.D., Philip E. LeBoit, M.D., Dan Pinkel, Ph.D., and Boris C. Bastian, M.D. Distinct Sets of Genetic Alterations in Melanoma. *The New England Journal of Medicine*. November 17, 2005
- [21] van 't Veer LJ, Burgering BM, Versteeg R, Boot AJ, Ruiter DJ, Osanto S, et al. N-ras mutations in human cutaneous melanoma from sun-exposed body sites. *Mol Cell Biol*. 1989 Jul;9(7):3114-6.
- [22] Dhawan P, Singh AB, Ellis DL, Richmond A. Constitutive activation of Akt/protein kinase B in melanoma leads to up-regulation of nuclear factor-kappaB and tumor progression. *Cancer Res*. 2002 Dec 15;62(24):7335-42.
- [23] Delehedde M, Seve M, Sergeant N, Wartelle I, Lyon M, Rudland PS, et al. Fibroblast growth factor-2 stimulation of p42/44MAPK phosphorylation and IkappaB degradation is regulated by heparan sulfate/heparin in rat mammary fibroblasts. *J Biol Chem*. 2000 Oct 27;275(43):33905-10.
- [24] Satyamoorthy K, Muylers J, Meier F, Patel D, Herlyn M. Mel-CAM-specific genetic suppressor elements inhibit melanoma growth and invasion through loss of gap junctional communication. *Oncogene*. 2001 Aug 2;20(34):4676-84.
- [25] Thomas L Hocker MKS. (*Journal of Investigative Dermatology* 2008).
- [26] Ornitz DM, Xu J, Colvin JS, McEwen DG, MacArthur CA, Coulier F, et al. Receptor specificity of the fibroblast growth factor family. *J Biol Chem*. 1996 Jun 21;271(25):15292-7.
- [27] Horton AC, Mahadevan NR, Ruvinsky I, Gibson-Brown JJ. Phylogenetic analyses alone are insufficient to determine whether genome duplication(s) occurred during early vertebrate evolution. *J Exp Zool B Mol Dev Evol*. 2003 Oct 15;299(1):41-53.
- [28] Christine Heinzle, Hedwig Sutterlüty Michael Grusch, Bettina Grasl-Kraupp,, Marian WBB. Targeting fibroblast-growth factor-receptor-dependentsignaling for cancer therapy. review. 2011.
- [29] Sekine K, Ohuchi, H., Fujiwara, M., Yamasaki, M., Yoshizawa, T., Sato, T., Yagishita, N., Matsui, D., Koga, Y., Itoh, N. & Kato, S. (1999). Fgf10 is essential for limb and lung formation. *Nat Genet*, 21, 138-41.
- [30] Beenken A, Mohammadi M. The FGF family: biology, pathophysiology and therapy. *Nat Rev Drug Discov*. 2009 Mar;8(3):235-53.
- [31] Mohammadi M, Honegger AM, Rotin D, Fischer R, Bellot F, Li W, et al. A tyrosine-phosphorylated carboxy-terminal peptide of the fibroblast growth factor receptor (Fg) is a binding site for the SH2 domain of phospholipase C-gamma 1. *Mol Cell Biol*. 1991 Oct;11(10):5068-78.
- [32] christine Wüchner KH, Bernhard Zabel and A. Winterpacht. Human fibroblast growth factor receptor 3 gene (FGFR3): genomic sequence and primer set information for gene analysis March 1997.
- [33] Mistry N, Harrington W, Lasda E, Wagner EJ, Garcia-Blanco MA. Of urchins and men: evolution of an alternative splicing unit in fibroblast growth factor receptor genes. *Rna*. 2003 Feb;9(2):209-17.
- [34] Ornitz DM, Itoh, N. . Fibroblast growth factors. review. 2001.
- [35] Ago H, Kitagawa Y, Fujishima A, Matsuura Y, Katsube Y. Crystal structure of basic fibroblast growth factor at 1.6 Å resolution. *J Biochem*. 1991 Sep;110(3):360-3.
- [36] Zhang JD, Cousens LS, Barr PJ, Sprang SR. Three-dimensional structure of human basic fibroblast growth factor, a structural homolog of interleukin 1 beta. *Proc Natl Acad Sci U S A*. 1991 Apr 15;88(8):3446-50.
- [37] Basilico C, Moscatelli D. The FGF family of growth factors and oncogenes. *Adv Cancer Res*. 1992;59:115-65.

- [38] Naski MC, Ornitz DM. FGF signaling in skeletal development. *Front Biosci.* 1998;3:d781-94.
- [39] Martin GR. The roles of FGFs in the early development of vertebrate limbs. *Genes Dev.* 1998 Jun 1;12(11):1571-86.
- [40] Crossley PH, Martinez S, Martin GR. Midbrain development induced by FGF8 in the chick embryo. *Nature.* 1996 Mar 7;380(6569):66-8.
- [41] Crossley PH, Minowada G, MacArthur CA, Martin GR. Roles for FGF8 in the induction, initiation, and maintenance of chick limb development. *Cell.* 1996 Jan 12;84(1):127-36.
- [42] Ye W, Shimamura K, Rubenstein JL, Hynes MA, Rosenthal A. FGF and Shh signals control dopaminergic and serotonergic cell fate in the anterior neural plate. *Cell.* 1998 May 29;93(5):755-66.
- [43] Allerstorfer S, Sonvilla G, Fischer H, Spiegl-Kreinecker S, Gauglhofer C, Setinek U, et al. FGF5 as an oncogenic factor in human glioblastoma multiforme: autocrine and paracrine activities. *Oncogene.* 2008 Jul 10;27(30):4180-90.
- [44] Zhan X, Bates B, Hu XG, Goldfarb M. The human FGF-5 oncogene encodes a novel protein related to fibroblast growth factors. *Mol Cell Biol.* 1988 Aug;8(8):3487-95.
- [45] Goldfarb M, Bates B, Drucker B, Hardin J, Haub O. Expression and possible functions of the FGF-5 gene. *Ann N Y Acad Sci.* 1991;638:38-52.
- [46] Bates B, Hardin J, Zhan X, Drickamer K, Goldfarb M. Biosynthesis of human fibroblast growth factor-5. *Mol Cell Biol.* 1991 Apr;11(4):1840-5.
- [47] Chambers SM FC, Papapetrou EP, Tomishima M, , Sadelain M SL. Highly efficient neural conversion of human ES and iPS cells by dual inhibition of SMAD signaling. 2009.
- [48] Fasano CA, Studer L. Too much Sonic, too few neurons. *Nat Neurosci.* 2009 Feb;12(2):107-8.
- [49] XI ZHAN BB, XIAOGAO HU, AND MITCHELL GOLDFARB. 18 march 88.
- [50] Dan Lindholm JH, Maria da Penha Berzaghi, Eero Castrén, Georgios Tzimogiorgis, Richard A. Hughes, Hans Thoenen. Fibroblast Growth Factor-5 Promotes Differentiation of Cultured Rat Septal Cholinergic and Raphe Serotonergic Neurons: Comparison with the Effects of Neurotrophins. *European journal of neuroscience.* April 2006.
- [51] Abuharheid S, Czubayko F, Aigner A. The fibroblast growth factor-binding protein FGF-BP. *Int J Biochem Cell Biol.* 2006;38(9):1463-8.
- [52] Antoine M, Wirz W, Tag CG, Gressner AM, Wycislo M, Muller R, et al. Fibroblast growth factor 16 and 18 are expressed in human cardiovascular tissues and induce on endothelial cells migration but not proliferation. *Biochem Biophys Res Commun.* 2006 Jul 21;346(1):224-33.
- [53] Boilly B, Vercoutter-Edouart AS, Hondermarck H, Nurcombe V, Le Bourhis X. FGF signals for cell proliferation and migration through different pathways. *Cytokine Growth Factor Rev.* 2000 Dec;11(4):295-302.
- [54] Johnson DE WL, Res AC. Structural and functional diversity in the FGF receptor multigene family. *Adv Cancer Res.* 1993.
- [55] Powers CJ, McLeskey SW, Wellstein A. Fibroblast growth factors, their receptors and signaling. *Endocr Relat Cancer.* 2000 Sep;7(3):165-97.
- [56] A. Orr-Urtreger MTB, T. Burakova, E. Arman, Y. Zimmer, A. Yayon, D. Givol and P. Lonai, . Developmental localization of the splicing alternatives of fibroblast growth factor receptor-2 (FGFR2). 1993.
- [57] Yan G, Fukabori Y, McBride G, Nikolaropolous S, McKeehan WL. Exon switching and activation of stromal and embryonic fibroblast growth factor (FGF)-FGF receptor

- genes in prostate epithelial cells accompany stromal independence and malignancy. *Mol Cell Biol*. 1993 Aug;13(8):4513-22.
- [58] Klint P, Claesson-Welsh L. Signal transduction by fibroblast growth factor receptors. *Front Biosci*. 1999 Feb 15;4:D165-77.
 - [59] Acevedo VD, Ittmann M, Spencer DM. Paths of FGFR-driven tumorigenesis. *Cell cycle* (Georgetown, Tex. 2009 Feb 15;8(4):580-8.
 - [60] Wagata T, Ishizaki K, Imamura M, Shimada Y, Ikenaga M, Tobe T. Deletion of 17p and amplification of the int-2 gene in esophageal carcinomas. *Cancer Res*. 1991;51(8):2113-
 - [61] Zammit C, Coope R, Gomm JJ, Shousha S, Johnston CL, Coombes RC. Fibroblast growth factor 8 is expressed at higher levels in lactating human breast and in breast cancer. *Br J Cancer*. 2002;86(7):1097-103.
 - [62] Valve EM, Nevalainen MT, Nurmi MJ, Laato MK, Martikainen PM, Harkonen PL. Increased expression of FGF-8 isoforms and FGF receptors in human premalignant prostatic intraepithelial neoplasia lesions and prostate cancer. *Lab Invest*. 2001;81(6):815-26.
 - [63] Kiuru-Kuhlefelt S, Sarlomo-Rikala M, Larramendy ML, Soderlund M, Hedman K, Miettinen M, et al. FGF4 and INT2 oncogenes are amplified and expressed in Kaposi's sarcoma. *Mod Pathol*. 2000;13(4):433-7.
 - [64] Ellen Margrethe Haugsten AW, Sjur Olsnes and Jørgen Wesche. Roles of Fibroblast Growth Factor Receptors in Carcinogenesis. American Association for Cancer Research. 2010.
 - [65] Taylor JGt, Cheuk AT, Tsang PS, Chung JY, Song YK, Desai K, et al. Identification of FGFR4-activating mutations in human rhabdomyosarcomas that promote metastasis in xenotransplanted models. *J Clin Invest*. 2009 Nov;119(11):3395-407.
 - [66] Avet-Loiseau H, Li JY, Godon C, Morineau N, Daviet A, Harousseau JL, et al. P53 deletion is not a frequent event in multiple myeloma. *Br J Haematol*. 1999 Sep;106(3):717-9.
 - [67] Presta M, Dell'Era P, Mitola S, Moroni E, Ronca R, Rusnati M. Fibroblast growth factor/fibroblast growth factor receptor system in angiogenesis. *Cytokine Growth Factor Rev*. 2005 Apr;16(2):159-78.
 - [68] Kornmann M, Ishiwata T, Beger HG, Korc M. Fibroblast growth factor-5 stimulates mitogenic signaling and is overexpressed in human pancreatic cancer: evidence for autocrine and paracrine actions. *Oncogene*. 1997 Sep 18;15(12):1417-24.
 - [69] Hanada K, Perry-Lalley DM, Ohnmacht GA, Bettinotti MP, Yang JC. Identification of fibroblast growth factor-5 as an overexpressed antigen in multiple human adenocarcinomas. *Cancer Res*. 2001 Jul 15;61(14):5511-6.
 - [70] Reuss B, von Bohlen und Halbach O. Fibroblast growth factors and their receptors in the central nervous system. *Cell and tissue research*. 2003 Aug;313(2):139-57.
 - [71] Grose R, Dickson C. Fibroblast growth factor signaling in tumorigenesis. *Cytokine Growth Factor Rev*. 2005 Apr;16(2):179-86.
 - [72] Halaban R, Kwon BS, Ghosh S, Delli Bovi P, Baird A. bFGF as an autocrine growth factor for human melanomas. *Oncogene research*. 1988 Sep;3(2):177-86.
 - [73] Metzner T. Evaluation of Fibroblast Growth Factor Receptors as Therapeutic Targets in Melanoma. diploma thesis. 2010.
 - [74] Pirker CH, Klausb; Spiegl-Kreinecker, Sabine; Elbling, Leonillaa; Thallinger, Christiane; Pehamberger, Hubert; Micksche, Michaela; Berger, Waltera. Chromosomal imbalances in primary and metastatic melanomas: over-representation of essential telomerase genes. a journal for basic translational and clinical research in melanoma. October 2003

- [75] Phelan MC. Basic techniques in mammalian cell tissue culture. Curr Protoc Cell Biol, Chapter 1, Unit 1 1 (2007).
- [76] Gallagher SRO-dSgeop. One-dimensional SDS gel electrophoresis of proteins. Curr Protoc Cell Biol, Chapter 6, Unit 6 1 2007.
- [77] Gallagher S, Winston, S.E., Fuller, S.A. & Hurrell, J.G. . Immunoblotting and immunodetection. Curr Protoc Immunol, Chapter 8, Unit 8 1 2008.
- [78] Gurtu V, Yan, G. & Zhang, G. (1996). I. IRES bicistronic expression vectors for efficient creation of stable mammalian cell lines. Biochem Biophys Res Commun, 229, 295-8. (1996).
- [79] (Andrew H. Fischer KAJ, Jack Rose, and Rolf Zeller,. Hematoxylin and Eosin Staining of Tissue and Cell Sections. 2008.
- [80] Takahashi JA, Fukumoto M, Igarashi K, Oda Y, Kikuchi H, Hatanaka M. Correlation of basic fibroblast growth factor expression levels with the degree of malignancy and vascularity in human gliomas. J Neurosurg. 1992 May; 76(5):792-8.
- [81] Wagata T, Ishizaki K, Imamura M, Shimada Y, Ikenaga M, Tobe T. Deletion of 17p and amplification of the int-2 gene in esophageal carcinomas. Cancer Res. 1991;51(8):2113-7.
- [82] Zammit C, Coope R, Gomm JJ, Shousha S, Johnston CL, Coombes RC. Fibroblast growth factor 8 is expressed at higher levels in lactating human breast and in breast cancer. Br J Cancer. 2002; 86(7):1097-103.
- [83] Valve EM, Nevalainen MT, Nurmi MJ, Laato MK, Martikainen PM, Harkonen PL. Increased expression of FGF-8 isoforms and FGF receptors in human premalignant prostatic intraepithelial neoplasia lesions and prostate cancer. Lab Invest. 2001; 81(6):815-26.
- [84] Kiuru-Kuhlefelt S, Sarlomo-Rikala M, Larramendy ML, Soderlund M, Hedman K, Miettinen M, et al. FGF4 and INT2 oncogenes are amplified and expressed in Kaposi's sarcoma. Mod Pathol. 2000; 13(4):433-7.
- [85] Halaban R, Langdon R, Birchall N, Cuono C, Baird A, Scott G, et al. Basic fibroblast growth factor from human keratinocytes is a natural mitogen for melanocytes. J Cell Biol. 1988 Oct;107(4):1611-9.
- [86] Johanna K. Ruohola TPV, Eeva M. Valve, Jani A. Seppä'n, Niina T. Loponen, Jaakko J. Keskitalo,, Päivi T. Lakkakorpi aPLHrn. Enhanced Invasion and Tumor Growth of Fibroblast Growth Factor 8b-overexpressing MCF-7 Human Breast Cancer Cells1. American Association for Cancer Research. May 15, 2001].
- [87] Ruff ARaE. Fibroblast Growth Factor Induces the Soft Agar Growth of Two Non-Transformed Cell Lines. Society for In Vitro Biology 1986.
- [88] Birck A, Kirkin AF, Zeuthen J, Hou-Jensen K. Expression of basic fibroblast growth factor and vascular endothelial growth factor in primary and metastatic melanoma from the same patients. Melanoma Res. 1999 Aug;9(4):375-81.
- [89] Li H-CWaP-C. Proteins Expressed on Tumor Endothelial Cells as Potential Targets for Anti-Angiogenic Therapy institute of Cellular and Organismic Biology, Academia Sinica, Taipei 115, Taiwan Journal of Cancer Molecules 4(1): 17-22, . 2008.
- [90] François G PC, Woerdenbag H, van Looveren M. . Antiplasmodial activities and cytotoxic effects of aqueous extracts and sesquiterpene lactones from *Neurolaena lobata* lanta Med 62:126–129. 1996.
- [91] Unger Christine MC. Extracts of anti-malarial and anti-inflammatory healing plants as oncolytic concept“ Diploma thesis. Wien, Oktober 2010.

6.5 Curriculum Vitae

Sara Ghassemi

Untereaugartenstraße Nr.31, Top 625

1020 Wien

Austria

E-mail: Sara_ghassemi@yahoo.com

Iranian Citizen

Date of Birth: 18.05.1983

EDUCATION

1990 – 1995 Primary School in Tehran

1995 – 1998 Secondary School in Tehran

1998 – 2000 High School (Matura in Experimental Sciences) in Tehran

2000 – 2001 Completion of Pre-University Course

2001 – 2002 Biology at Azad University of Tehran

2002 – 2003 Preliminary Study Course at University of Vienna (German course)

Since 10/2003 Studying Genetics and Microbiology at the University of Vienna

Specialization: Molecular Medicine, Immunology, Pathology and Genetics

WORK / RESEARCH EXPERIENCE

Since 02/2010 Medical University of Vienna

Department of Medicine I; Institute of Cancer Research (Group: Michael Grusch)

PROJECT

Over-expression of Fibroblast Growth Factor 5 (FGF5) in Melanoma:

Evaluation of its Role in Tumor Progression and Potential Therapeutic Implications

PUBLICATION

Fibroblast Growth Factor Receptors as Therapeutic Targets in Human Melanoma:
Synergism with BRAF Inhibition

Thomas Metzner¹, Alexandra Bedeir¹, Gerlinde Held¹, Barbara Peter-Vörösmarty¹, **Sara Ghassemi**¹, Christine Heinzle¹, Sabine Spiegl-Kreinecker², Brigitte Marian¹, Klaus Holzmann¹, Bettina Grasl-Kraupp¹, Christine Pirker¹, Michael Micksche¹, Walter Berger¹, Petra Heffeter¹ and Michael Grusch¹

LANGUAGES

Persian: Native speaker

German: Fluently spoken and written

English: Advanced